catalysts

MDPI

Article

Niobium and Zirconium phosphates as green and water-tolerant catalysts for the acid-catalyzsed valorizsation of bio-based chemicals and real lignocellulosic biomasses

Claudia Antonetti [1,2,*], Anna Maria Raspolli Galletti [1,2], Domenico Licursi [1,2], Sara Fulignati [1,2], Nicola Di Fidio [1,2], Federica Zanetti [3], Andrea Monti [3], Tommaso Tabanelli [4],Fabrizio Cavani [4]

[1] Department of Chemistry and Industrial Chemistry, University of Pisa, Via Giuseppe Moruzzi 13, 56124, Pisa, Italy, claudia.antonetti@unipi.it, anna.maria.raspolli.galletti@unipi.it, domenico.licursi@unipi.it, sara.fulignati@dcci.unipi.it, nicola.difidio@unipi.it
[2] Consorzio Interuniversitario Reattività Chimica e Catalisi (CIRCC), Via Celso Ulpiani 27, 70126, Bari, Italy.
[3] Department of Agricultural and Food Sciences, University of Bologna, Viale G. Fanin 44, Bologna, 40127, Italy, federica.zanetti5@unibo.it, a.monti@unibo.it
[4] Department of Industrial Chemistry "Toso Montanari", Alma Mater Studiorum University of Bologna, Viale Risorgimento 4, 40136, Bologna, Italy, tommaso.tabanelli@unibo.it, fabrizio.cavani@unibo.it
* Correspondence: claudia.antonetti@unipi.it; Tel.: +390502219329.

Abstract: Commercial niobium and synthesized zirconium phosphates were~~have been~~ tested as water~~-~~tolerant heterogeneous acid catalysts in the hydrothermal conversion of different bio-based substrates. Different acid-catalyz~~s~~ed reactions were performed using~~, on both~~ biomass-derived model compounds and more complex real lignocellulosic biomasses, as the substrate~~have been carried out~~. The conversion of glucose and cellulose was preliminarily investigated~~,~~ T~~t~~hen~~, moving then toward~~ a wide plethora of raw lignocellulosic biomasses, such as conifer wood sawdust, Jerusalem artichoke, sorghum, miscanthus, foxtail millet, hemp and *Arundo donax*, was valorized towards~~ addressed at~~ the production of water-soluble saccharides, 5-hydroxymethylfurfural (HMF), levulinic acid (LA) and furfural. The different catalytic performances of~~for~~ the two phosphates were explained~~justified~~ on the basis of their acid features, total acidity, ~~the~~ Brønsted/Lewis acid sites ratio and strength. Moreover, a~~, gaining~~ better insight ~~of~~ on their structure-acidity relationship was proposed. The different acid properties of niobium and zirconium phosphates has ~~enables~~ enabled us to tune the reaction towards the target product/s, achieving respectively, from glucose, maximum HMF and LA yields of 24.4 and 24.0 mol%~~,~~ respectively, starting from glucose~~working at 160 °C~~. ~~Moreover~~Remarkably, when real Jerusalem artichoke biomass~~es~~ was~~are~~ adopted, ~~starting from Jerusalem artichoke,~~ working in the presence of niobium and zirconium phosphate ~~respectively~~, maximum yields to furanic compounds ~~of 12.7 mol%~~ and to cellulose derived sugars of 12.7 and 50.0 mol%, respectively, were obtained~~, respectively,~~ after only 1 h of reaction. ~~Finally, t~~The synthesized~~achieved~~ hydrolysates, resulting rich in C5 and C6 carbohydrates,~~sugars and oligomers, result suitable~~ will be better exploited for the cascade production of more added-value bio-products ~~subsequent valorization, according to cascade processes~~.

Keywords: niobium phosphate; zirconium phosphate; lignocellulosic biomasses, 5-hydroxymethylfurfural, levulinic acid, ~~furfural, cellulose and hemicellulose derived~~ sugars, ~~cellulose and hemicellulose derived~~ oligomers~~, heterogeneous catalyzed biomass conversion~~.

Citation: Lastname, F.; Lastname, F.; Lastname, F. Title. *Catalysts* **2022**, *12*, x. https://doi.org/10.3390/xxxxx

Academic Editor: Firstname Lastname

Received: date
Accepted: date
Published: date

Publisher's Note: MDPI stays neutral with regard to jurisdictional claims in published maps and institutional affiliations.

1. Introduction

Emerging economies with political and environmental concerns about fossil fuels have spurred research into utilizing biomass as feedstock for the sustainable production of new fuels and chemicals. 5-hydroxymethylfurfural (HMF) [1,2~~-4~~7] and levulinic acid (LA) [3,4~~5~~8~~-9~~14] are very versatile platform chemicals, usable as building-blocks for the

synthesis of many added-value bio-fuels [5,6] and bio-chemicals [7,8~~10~~~~5~~ 15~~22~~]. Hydrothermal production of HMF and/or LA from lignocellulosic biomasses involves a multi-step complex reaction sequence, which, once glucose is formed by the hydrolysis stage, includes: i) isomerization of glucose to fructose, ii) fructose dehydration to HMF, and iii) HMF ring opening by hydrolysis to LA. In this context, many side-reactions occur, mainly condensations of furanic compounds to give low-molecular water-soluble and higher-molecular water-insoluble humins [9,10~~16~~~~23~~ 18~~25~~]. Formic acid (FA) is co-produced in equimolar amount, or even slightly higher than LA within LA synthesis, in this latter case due to the possible side reactions of reactive intermediates [11,12~~9~~~~26~~,~~207~~]. The general pathway of the involved reactions, starting from glucose, is reported in Scheme 1.

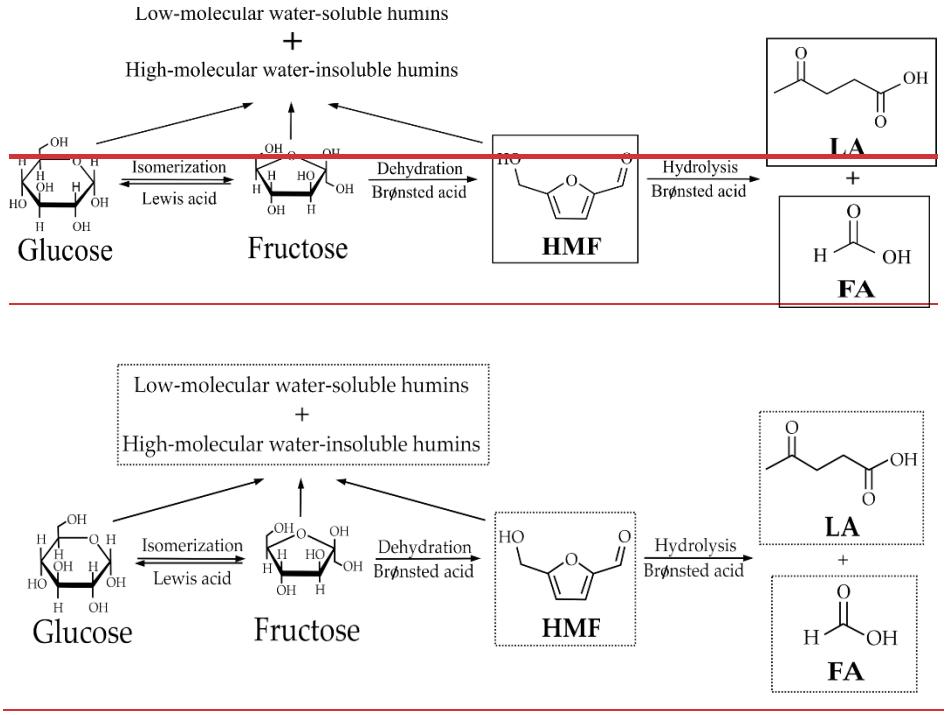

Scheme 1: Reaction pathway of isomerization/dehydration/hydrolysis reactions from glucose to HMF and LA/FA, highlighting the roles of Brønsted/Lewis acids.

~~As shown in the above scheme,~~ Eeach of these reactions ~~(isomerization, dehydration and hydrolysis)~~ behaves differently, depending on the type and strength of the acid catalyst. ~~In particular,~~ Lewis acids selectively favor the first isomerization step of glucose to fructose, whereas Brønsted acids enable the subsequent dehydration/hydrolysis reactions [2,13,14~~36~~,~~ 21~~8~~ 25~~32~~]. Therefore, HMF synthesis requires an accurate tuning ~~and balancing~~ both of ~~the~~ Brønsted/Lewis acidity and ~~the~~ strength of their acid sites, together with mild reaction conditions of temperature and time, whereas the subsequent HMF hydrolysis to LA needs Brønsted sites and harsher reaction conditions [15,16~~26~~~~33~~ 28~~35~~]. Focusing on HMF production, this compound is traditionally synthesized starting from syrups extracted from energy crops, adopting homogeneous catalysts, followed by a liquid/liquid extraction with organic solvents [17~~29~~~~36~~]. In a similar way, LA production~~,~~ traditionally~~,~~ involves the use of strong inorganic acids, such as HCl and H_2SO_4, as homogeneous catalysts of a two-stage process where~~,~~ LA is first produced and then recovered by stripping ~~after the production of LA in the first step, the second one works as a stripping column to remove by-products and recover LA~~ [48~~12~~]. For both HMF and LA processes, the difficult recovery of the homogeneous catalyst, ~~the~~ disposal problems and ~~, along with~~ equipment corrosion issues, make heterogeneous systems certainly more attractive~~interesting~~ for industrial applications. Nevertheless, ~~up to now,~~ few examples of heterogeneous catalysts

for HMF and LA production have been reported in the literature, such as ~~the majority of them starting from model compounds. The most studied ones~~ are metal oxides, carbon-based catalysts, zeolites, metal organic frameworks (MOF), resins and metal phosphates [1,2~~3~~6]. ~~Among them,~~ M~~m~~etal oxides [1,18~~3~~07] ~~usually~~ have low activity and need organic solvents ~~as the reaction medium~~, leading to environmental and economic drawbacks ~~the non-environmental choices and high costs of the catalytic system~~. Similarly, carbon-based catalysts [1,193~~1~~8] ~~often~~ show low ~~reaction~~ activity and selectivity, as well as, ~~in addition to the presence of side reactions and~~ poor stability~~le pore structure,~~ resulting in ~~the~~ easy leaching of the active component(s). On the other hand, zeolites have ~~are characterized by~~ a good thermal stability, but undergo ~~the common problems limiting their utilization in biomass transformation are is their catalytic~~ deactivation by pore blockage, as a consequence of the precipitation of various reaction by-products on their surfaces~~caused by the formation of humins products, leading to pore blockage~~. Moreover, zeolite systems [1,203~~2~~9] generally undergo metal leaching ~~are easy to leach metals from the zeolite framework when the reactions are carried out~~ in the aqueous phase, thus resulting quite unstable for these applications~~requiring the use of many organic solvents for practical application, which not only increases the cost of wet catalytic system, but also causes environmental pollution~~. MOFs exhibit high porosity and better tunable reactivity than zeolites, at the same time requiring simpler synthesis procedures~~, adjustable functionality and rich~~ rich metal centers with a porous structure similar to that of zeolite but easier to prepare than zeolite analogues and their chemical catalysis is easier to tune. ~~However~~ Despite these relevant advantages, ~~also MOFs exhibit some unsolved drawbacks: in fact, their functionalization requires a lot of significant work and they are characterized by~~ synthesized MOFs still show ~~a~~ poor ~~hydrothermal and~~ thermochemical stability, due to the weak coordination bond of the bridged metal ~~coordination bond bridged by MOF~~ [1,213~~3~~40]. Acid resins ~~are~~ generally show~~characterized by~~ higher catalytic performances than the above mentioned catalysts, but their satisfactory recycling is still difficult to achieve, ~~even if they show low surface area, which can adversely affect the recycle of the catalysts, often requiring organic solvents~~, thus making their industrial application still unfeasible [1,223~~4~~41]. Finally, metal phosphates, in particular niobium and zirconium phosphates (NbPO and ZrPO), appear promising systems, ~~because they~~ keeping their strong acidic properties even in polar liquids, as ~~including~~ water and~~, also~~ at high temperatures. Remarkably, ~~and~~ these catalysts~~ey~~ can be easily reactivated by simpler thermal treatments [2~~3~~6].

~~In this context, regarding HMF production, the catalytic performances of niobium phosphate (NbPO) and zirconium phosphate (ZrPO) towards isomerization/dehydration/hydrolysis reactions starting from model sugars have been investigated, taking into consideration some remarkable advantages, in particular their high thermal stability and good water tolerance [6,42–55]. In this perspective, Ordomsky et al. studied the catalytic performances of various synthesized metal phosphates in glucose transformation to HMF, whose performances followed the order: aluminium < titanium < zirconium < niobium phosphates, in agreement with the increase of the strength of their acid sites [53]. The highest HMF selectivity (56 mol% at 20 mol% glucose conversion) was obtained adopting a synthesized NbPO with a balanced ratio Brønsted/Lewis acid sites equal to 1, working at 135°C with a glucose loading of 6.2 wt%, while an excess of Lewis acid sites caused the excessive formation of undesired humins, leading to significant catalyst deactivation. The authors proposed that the synergism between a protonated phosphate group and a nearby metal Lewis acid site in the two-stage glucose transformation into HMF leads to a highly selective glucose isomerization/dehydration, whereas an excess of Lewis acidity led to the undesired conversion of glucose into humins, decreasing the selectivity to HMF. These considerations on the Brønsted/Lewis acidity of the phosphates derive from FT-IR experiments carried out through adsorption of pyridine, but the authors do not consider the effect of the water medium on the catalytic properties of the phosphates to give HMF. In this perspective, Antonetti et al. [6] studied the Brønsted/Lewis acidity of NbPO and ZrPO when pyridine and water were co-adsorbed and compared the achieved results to the case of pyridine-only adsorption. Working under hydrous conditions the authors proved that a significant increase of the Brønsted/Lewis ratio occurred for NbPO system, whereas only a minor variation of the Brønsted/Lewis intensity ratio was observed in the case of ZrPO. Moreover, the new Brønsted sites generated by water adsorption for NbPO were characterized by a comparatively higher acidity, making this system (under hydrous conditions) a strong Brønsted-type acid system. On the other hand,~~

~~under the same hydrous conditions, ZrPO acid sites remained mainly of the Lewis type together with Brønsted sites of comparatively lower strength, changing little its acid features. In another work, again in the context of model compounds, Weingarten et al. [32] employed ZrPO for the conversion of glucose to HMF, obtaining at 160°C the highest HMF yield of only 15 mol%, together with significant amount of humins. The formation of humins is also confirmed by the study of De Jesus Junior et al. [42], which investigated the conversion of glucose to HMF in the presence of NbPO, where the highest HMF yield of 15 mol% was obtained at 145°C after 3h of reaction. Better results were obtained in the work of Zhang et al. [51], who synthesized a series of porous niobium phosphates at different pH values, in order to tune the surface acidity and the ratio of Brønsted/Lewis acid sites. It was found that an excess of Brønsted acid sites could inhibit the isomerization of glucose to fructose, which is a Lewis acid promoted process, but boosts the subsequent fructose conversion. On the other hand, an excess of Lewis acidity has a negative influence on the dehydration of fructose, which would lead to undesired side reactions to give humins [29,51]. NbPO prepared at pH=7 showed the best catalytic performances, achieving HMF selectivity up to 50 mol%, starting from glucose under the best reaction conditions. In addition, this synthesized catalyst exhibited excellent stability, with almost no decrease in activity and/or selectivity, even after seven successive runs [51]. Finally, Saravanan et al. [54] studied the effect of calcination temperature, in the range 500-800°C, on the Brønsted/Lewis acid properties of a large-pore mesoporous ZrPO synthesized by hydrothermal path in the conversion of glucose to HMF. The authors found that the conversion of glucose decreased with increasing the calcination temperatures, with a significant worsening of the catalytic performances to HMF at calcination temperatures higher than 600 °C. This latter temperature was optimal for HMF production (HMF selectivity up to 53 mol%), allowing a good balance between Brønsted and Lewis acid sites. In another work, the NbPO calcinated at 600°C was adopted for the conversion of cellobiose to HMF achieving at 140°C after 10 minutes a HMF yield of about 6 mol% [43].~~

~~Regarding LA production, the same considerations for HMF can be carried out, taking into account that up to now, few heterogeneous catalysts have been used for its synthesis, limiting their use to ideal and model feedstocks, such as soluble sugars or clean cellulose, rather than real lignocellulosic biomasses [12]. In this context, heterogeneous acid catalysts have been used for the synthesis of LA from fructose, glucose, sucrose, starch and cellulose [56-63], obtaining yields of about 50 mol%, resulting well comparable with those achieved with homogenous systems. In particular, Tang et al. studied the production of LA starting from glucose, using graphene oxide with sulfonic acid groups as the acid catalyst, achieving the highest yield of 78 mol% [58]. A different catalyst was adopted by Hegner et al. who investigated Nafion SAC 13 for LA synthesis from the model cellulose, but achieving only a low LA yield (14 mol%), if used alone [64]. Interestingly, with the same catalyst, LA yield was significantly improved, up to 72 mol%, adding NaCl to the solution. The salt ions weaken the hydrogen bonding network of the cellulose structure, thus making it less recalcitrant for the reaction [62]. The use of metal phosphates for the production of LA is scarce, even starting from model compounds. Weingarten et al. studied the catalytic activity of zirconium and tin phosphates to produce LA from glucose. In particular, ZrPO with the P/Zr molar ratio of 2 resulted the best acid catalyst, achieving the highest LA yield of 14.0 mol% at 160°C [32].~~

~~Moving toward the employment of heterogeneous acid catalysts with real lignocellulosic biomasses for HMF and LA synthesis, satisfactory examples are uncommon due to many factors, such as the biomass nature which limits the effective interactions between the substrate and the active surface of the solid catalysts, diffusion limitations inside the catalyst pores etc. In this perspective, Parshetti et al. investigated the conversion of food waste biomass to HMF, reaching the maximum HMF yield of 4.3 weight % (the composition, in terms of cellulose amount, of the starting biomass is absent, so the achieved yield is reported as weight %) in the presence of ZrPO calcinated at 400°C after 6h of reaction [55]. For these reasons the use of heterogeneous catalysts for the conversion of real lignocellulosic biomasses requires preliminary pretreatment steps, which make the substrate more suitable for the subsequent reactions.~~

Up to now, few works reported the use of heterogeneous catalysts ~~have been used~~ for the synthesis of HMF and LA starting from real feedstocks and their employment is generally~~,~~ limited~~ting their use~~ to the conversion of ~~ideal and~~ model substrates~~feedstocks~~, such as soluble sugars or pure ~~clean~~ cellulose ~~, rather than real lignocellulosic biomasses~~ [~~48~~12]. In this context, ~~regarding HMF and LA production,~~ Table 1 summarizes the most relevant literature results on the catalytic performances of ~~niobium phosphate (~~NbPO~~)~~ and ~~zirconium phosphate (~~ZrPO ~~) reported in the literature works~~ towards~~–~~ HMF and

LA production in water, ~~isomerization/dehydration/hydrolysis reactions~~ starting from model sugars and/or real biomasses ~~[36,3542 5663]~~.

Table 1: Literature review on HMF and LA production in water catalyzed by NbPO and ZrPO (RAC = substrate/catalyst ratio wt/wt).

Catalyst	Substrate	Product	Reaction conditions	Product yield (mol%)	Reference
NbPO	Fructose	HMF	190 °C, 8 min, RAC 6 wt/wt, 10 wt% loading	32.2	[236]
NbPO	Fructose	HMF	130 °C, 60 min, RAC 1 wt/wt, 4.5 wt% loading	33.6	[234451]
NbPO	Glucose	HMF	145 °C, 180 min, RAC 3 wt/wt, 2 wt% loading	15.0	[243542]
NbPO	Glucose	HMF	140 °C, 60 min, RAC 1 wt/wt, 4.5 wt% loading	14.1	[234451]
NbPO	Glucose	HMF	135 °C, 390 min, RAC 2 wt/wt, 6.2 wt% loading	11.2	[254653]
NbPO	Cellobi-ose	HMF	140 °C, 10 min, RAC 10 wt/wt, 1 wt% loading	6.0	[23643]
ZrPO	Fructose	HMF	190 °C, 8 min, RAC 6 wt/wt, 10 wt% loading	39.4	[236]
ZrPO	Glucose	HMF	160 °C, 150 min, RAC 2 wt/wt, 10 wt% loading	15.0	[142532]
ZrPO	Glucose	HMF	155 °C, 360 min, RAC 2 wt/wt, 0.5 wt% loading	46.6	[274754]
ZrPO	Glucose	LA	160 °C, 150 min, RAC 2 wt/wt, 10 wt% loading	14.0	[142532]
ZrPO	Food waste	HMF	160°C, 360 min, RAC 2 wt/wt, 4 wt% loading	4.3[a]	[24855]

[a] yield expressed as weight % with respect to biomass dry weight due to the absence of the cellulose content in the biomass

I~~n this perspective, i~~n this work, the catalytic performances of ~~two different heterogeneous phosphates,~~ NbPO and ZrPO~~,~~ have been evaluated for several acid-catalyzed hydrolysis/isomerization/dehydration reactions, starting not only from the model ~~compounds~~ glucose and cellulose, but also from ~~the more complex~~ real lignocellulosic biomasses, such as conifer wood sawdust, Jerusalem artichoke, sorghum, miscanthus, foxtail millet, hemp and *Arundo donax*. In this context, the correlation between Brønsted/Lewis acidity of NbPO and ZrPO ~~with~~ and their catalytic performances has been investigated, especially clarifying ~~especially~~ the acidity role and structural modifications which~~of the~~ phosphates may undergo ~~when used~~occurring in the water mediuma~~queous media~~. Moreover, starting from glucose, the optimization of the ~~reaction towards the synthesis of~~ HMF or LA synthesis with ~~, adopting respectively~~ NbPO and ZrPO~~,~~ has been carried out~~, paying attention to the main reaction parameters affecting the product yields~~. On the other

hand, starting from raw lignocellulosic biomasses, and employing the same phosphates, it is possible to easily ~~deconstruct the matrix~~access the plant tissue, selectively produce~~ing~~ furanic compounds (HMF and furfural) or ~~cellulose~~ cellulose-derived sugars ~~with NbPO and ZrPO respectively, in very short reaction time, obtaining compounds readily~~ which can be further converted into ~~convertible in~~ a plethora of more added-value~~valuable~~ products~~compounds~~ ~~in~~ within the biomass supply chain. ~~In conclusion, t~~The proposed approach, in particular the employment of these phosphates for the one-pot conversion of low-cost substrates, represents a preliminary but necessary step towards the heterogeneously catalyzed biomass conversion, in the perspective of the development of these processes on a greater industrial scale. ~~and, to the best of our knowledge, this is the first research that reports the successful one-pot direct employment of these phosphates in water to give different value-added compounds and promising hydrolysates, rich in hemicellulose and cellulose sugars and oligomers, suitable for subsequent catalytic and/or biocatalytic valorization cascade processes.~~

2. Results and Discussion

2.1 Conversion of glucose in the presence of NbPO and ZrPO

Commercial NbPO and synthesized ZrPO were tested for the conversion of glucose in water. These systems are characterized ~~, taking into consideration that these systems are characterized~~ by the presence of both Brønsted and Lewis acid sites~~,~~ and they already were ~~previously~~ successfully adopted by ~~the same authors~~ us for the microwave (MW)-assisted dehydration of fructose and inulin to HMF [2~~3~~6]. Table 2~~1~~ summarizes the acid properties of NbPO and ZrPO under hydrous conditions, studied in the previous research [2~~3~~6].

Table 2~~1~~: Acid properties of NbPO and ZrPO under hydrous conditions [2~~3~~6].

	Total acidity (mmol/g)[a]	Brønsted/Lewis ratio[b]
NbPO	0.33	1.0
ZrPO	0.43	0.2

[a] determined by NH_3-TPD analysis; [b] values at 200 °C obtained from FT-IR spectra recorded at increasing temperature after room-temperature co-adsorption of pyridine and water.

The dehydration of fructose to HMF reaction requires Brønsted acidity, whereas both Lewis and Brønsted acidities are necessary when glucose is employed ~~needed adopting glucose~~ as substrate ~~starting model compound,~~ and their balance, in terms of number and strength of the acid sites, is of paramount importance. In fact, the transformation of glucose to HMF is characterized by a complex network of reactions, which are~~that are~~ differently promoted by Lewis or Brønsted acid sites. ~~,~~ On this basis, ~~thus resulting of particular interest~~ the study of the different ~~behaviours~~behaviors of these two systems in aqueous ~~media~~medium is of particular interest.

Firstly, the reaction has been investigated in the autoclave reactor ~~with traditional heating~~ at the temperature of 150 °C, adopting the glucose loading of 5 wt% and the glucose/catalyst weight ratio of 1.2, selected on the basis of preliminary tests (not reported). The obtained results are shown in Figure 1. NbPO shows higher glucose conversion than ZrPO and this can be justified considering that NbPO in aqueous media is characterized by a higher amount of Brønsted acid sites, which promote the dehydration/hydrolysis reaction. In particular, they can boost the fructose dehydration to HMF~~,~~ and, as consequence, foster ~~in this way~~thus ~~fostering~~ the isomerization equilibrium from glucose towards ~~to~~ fructose, thus improving the ~~resulting in higher~~ glucose conversion. Regarding the products distribution, at short reaction time, ~~while~~ NbPO shows a relatively high

selectivity and yield towards HMF, whereas ZrPO reveals a marked selectivity towards fructose. This can be explained considering ~~taking into consideration~~ the different type of catalysts acid properties ~~acid properties of the employed catalysts~~ [23~~6~~]. In fact, in water NbPO has fewer Lewis centers and a larger amount of Brønsted ones than ZrPO but all of them are characterized by high acid strength. ~~NbPO, if used in aqueous media, is characterized by a higher Brønsted/Lewis ratio than ZrPO, where for NbPO, both the fewer Lewis centers and the huger amount of Brønsted ones are characterized by high acid strength~~. The~~is~~ peculiar balance of these acid centers allows us to obtain the selective formation of HMF with NbPO. In fact,~~, because~~ the Lewis centers boost the isomerization of glucose to fructose, whereas the Brønsted ones ~~favour~~favor the subsequent dehydration of fructose to HMF.~~,~~ As consequence,~~ thus further enhancing~~ the isomerization of glucose to fructose is further enhanced and~~, allowing us to achieve~~ HMF selectivity ~~values~~ higher than 60 mol% is achieved at the beginning of the reaction (30 min~~.~~). On the other hand, ZrPO, under the same aqueous conditions, is characterized by a higher concentration of acid sites with a predominant Lewis nature (Table 2~~1~~), allowing a higher selectivity in fructose at the beginning of the reaction.

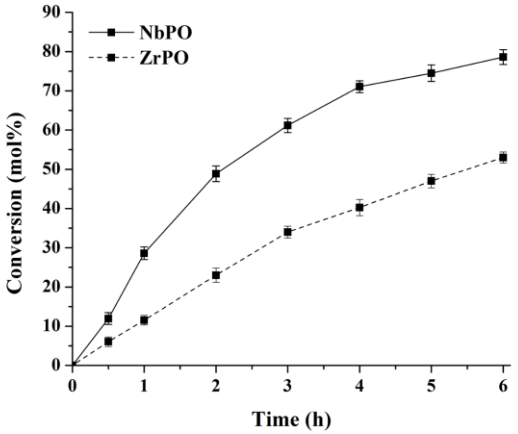
NbPO
ZrPO
Conversion (mol%)
Time (h)

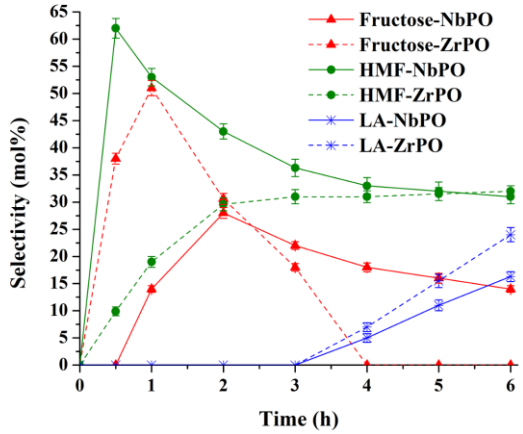
Fructose-NbPO
Fructose-ZrPO
HMF-NbPO
HMF-ZrPO
LA-NbPO
LA-ZrPO
Selectivity (mol%)
Time (h)

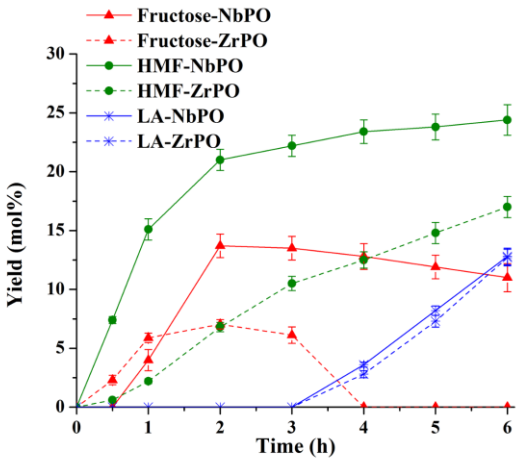
Fructose-NbPO
Fructose-ZrPO
HMF-NbPO
HMF-ZrPO
LA-NbPO
LA-ZrPO
Yield (mol%)
Time (h)

275

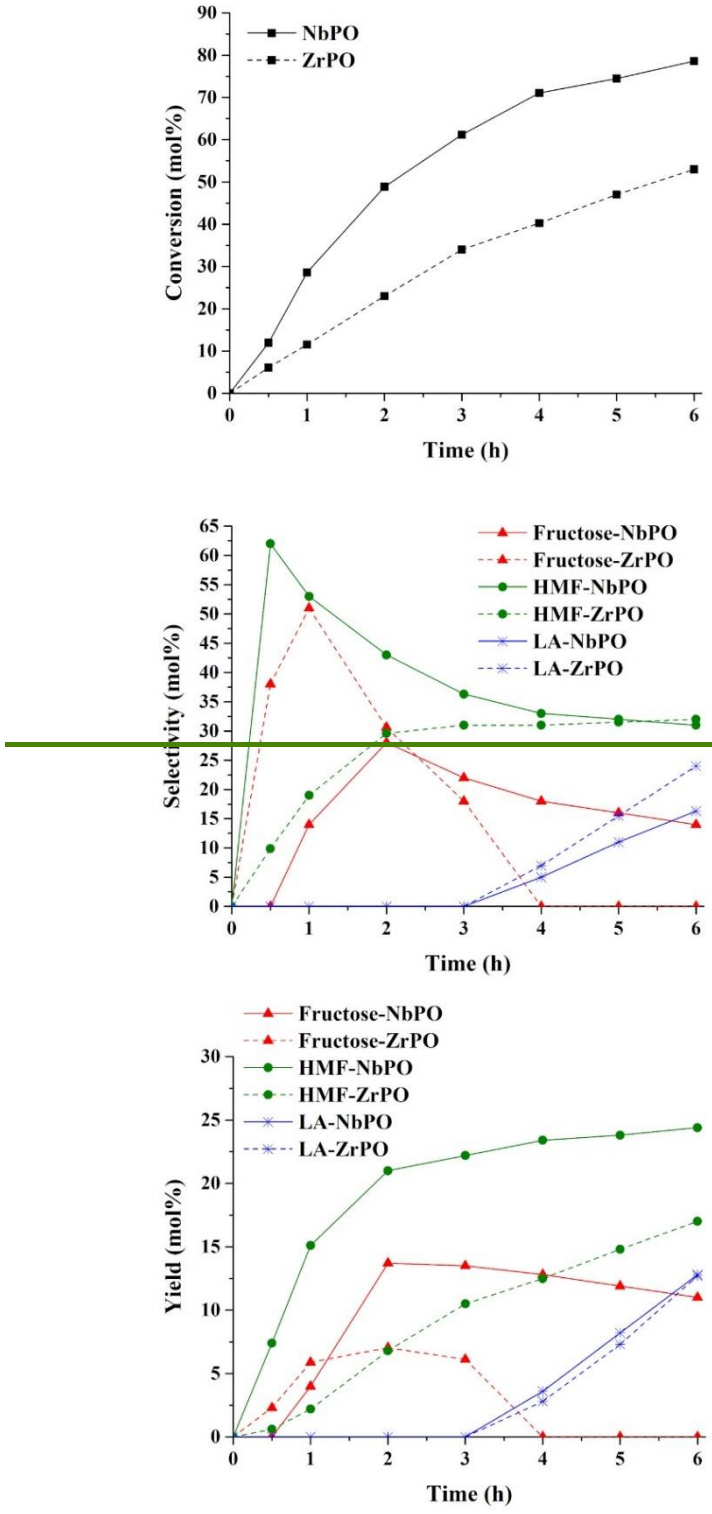

Figure 1: Glucose conversion in the presence of NbPO and ZrPO as acid catalysts in autoclave at 150 °C. Reaction conditions: glucose = 2.47 g; catalyst = 2.06 g; water = 47.0 g; T = 150 °C. (Note: where the error bars are not visible, they are smaller than the symbols).

Moreover, it is interesting to note the different ~~behaviour~~behavior of the two systems in the range 1-3 h.~~:~~ When NbPO is employed~~for NbPO~~, a significant decrease of HMF selectivity occurred without the simultaneous production of LA, thus indicating the

formation of humins, as confirmed by the corresponding lower %C recovered (mol%)~~carbon balance~~. On the other hand, in the presence of ZrPO, ~~in the same time range,~~ HMF selectivity ~~for ZrPO~~ increased~~s~~ and a~~, with~~ scarce production of humins took place, as confirmed by the higher %C recovered (mol%)~~carbon balance~~ for ZrPO (after 3 h, the %C recovered~~carbon balance~~ results 74.5 and 82.6 mol% for NbPO and ZrPO, respectively). For both phosphates, the prolonging of the reaction time ~~favours~~favors ~~for both phosphates~~ the conversion of HMF to LA, due to the presence of Brønsted acid sites, with comparable yields after 6 h of reaction (12.7 mol%). These results highlight ~~as~~ that the kinetics of NbPO and ZrPO are differen~~t~~t: NbPO is more active and more selective towards HMF at short~~er~~ reaction time, due to~~being characterized by~~ the equal amount of Brønsted and Lewis acid sites, ~~responsible for~~that promote the conversion of glucose to HMF through fructose. On the other hand~~,~~ ~~whereas the kinetics of~~ ZrPO, ~~is slower and~~ being characterized by a predominant Lewis acidity, led to a slower conversion and higher fructose selectivity at short reaction time ~~it results more selective to fructose at short reaction time at short reaction time~~. The achieved catalytic performances indicate the commercial NbPO as a suitable system for the production of HMF, reaching the HMF yield of 22.2 mol% after only 3 h of reaction and the highest HMF yield of 24.4 mol% after 6 h, values higher than those reported in the literature for analogous aqueous systems [1,23,24,293~~5~~~~42~~,37~~44~~,44~~51~~]. In fact, working in pure water, which leads to a high decomposition of the formed HMF [293744], Ordomsky et al. obtained HMF yields below 10 mol%, working with the same NbPO system at 135 °C, and adopting the glucose loading of 5 wt% [2546~~53~~]. ~~Moreover, t~~The same authors reached the highest selectivity to HMF equal to 56 mol% at 20 mol% glucose conversion, ~~that was achieved~~ in the presence of a synthesized NbPO with a Brønsted/Lewis acid sites ratio equal to 1 [2546~~53~~], the same acid ratio of the commercial NbPO adopted in our experimental conditions where the maximum HMF selectivity resulted 62.5 mol% at 11.9 mol% glucose conversion. Moreover, they studied the catalytic performances of various synthesized metal phosphates in glucose transformation to HMF, whose performances followed the order: aluminum < titanium < zirconium < niobium phosphates, in agreement with the increase of the strength of their acid sites. The excess of Lewis acid sites caused the excessive formation of undesired humins, leading to significant catalyst deactivation. The authors proposed that the synergism between a protonated phosphate group and a nearby metal Lewis acid site in the two-stage glucose transformation into HMF le~~ads~~d to a highly selective glucose isomerization/dehydration, whereas an excess of Lewis acidity ~~led to~~favored the undesired conversion of glucose into humins, decreasing the selectivity to HMF. These considerations on the Brønsted/Lewis acidity of the phosphates derive from FT-IR experiments carried out through adsorption of pyridine, but the authors do not consider the effect of ~~the~~ water ~~medium~~ on the catalytic properties of the phosphates ~~to give HMF~~. In this perspective, Antonetti et al. [2~~3~~6] studied the Brønsted/Lewis acidity of NbPO and ZrPO when pyridine and water were co-adsorbed and compared the achieved results to the case of pyridine-only adsorption. Working under hydrous conditions, the authors proved that a significant increase of the Brønsted/Lewis ratio occurred for NbPO system, whereas only a minor variation of the Brønsted/Lewis intensity ratio was observed ~~in the case of~~for ZrPO. Furthermore, the new Brønsted sites generated on NbPO surface by water adsorption ~~for NbPO~~ had comparatively higher strength~~were characterized by a comparatively higher acidity~~, thus making this system (under hydrous conditions) a strong Brønsted-type acid system. On the other hand, under the same hydrous conditions, ZrPO acid sites remained mainly of the Lewis type together with Brønsted sites of comparatively lower strength, changing ~~little~~ its acid features little. Comparable results to Ordomsky et al. were also obtained by De Jesus Junior et al. [243~~5~~~~42~~], who studied the conversion of 2 wt% aqueous solution of glucose to HMF in the presence of the commercial NbPO, achieving the highest HMF yield equal to 15 mol% at 145 °C after 3 h of reaction. Moving towards synthesized NbPO, higher HMF yields, up to 33.6 mol%, ~~can be~~were obtained from 4.8 wt% glucose aqueous solution in pure water, adopting a porous NbPO catalyst synthesized at pH=7, working at 140 °C for

1 h [2344~~51~~]. Moreover, it was found that an excess of Brønsted acid sites could inhibit the isomerization of glucose to fructose, which is a Lewis acid-promoted process, but boosts the subsequent fructose conversion. On the other hand, an excess of Lewis acidity has a negative influence on the dehydration of fructose, which would lead to undesired side reactions to give humins [13,23~~229~~,44~~51~~]. NbPO prepared at pH=7 showed the best catalytic performances, achieving HMF selectivity up to 50 mol%, starting from glucose, under the best reaction conditions. In addition, this synthesized catalyst exhibited excellent stability, with almost no decrease in activity and/or selectivity, even after seven successive runs [234~~4~~51]. On the other hand, ZrPO can be considered a promising catalyst for the production of LA thanks to ~~the catalytic performances of ZrPO, taking into account the best carbon balance and~~ its higher selectivity to LA compared to NbPO (Figure 1) and the %C recovered (mol%)~~., suggest that ZrPO as is a promising catalyst for the production of LA~~. Thus, in order to confirm this explanation and increase the production of LA, ZrPO was tested at 180 °C under the same reaction conditions, as reported in Figure 2.

~~The increase of temperature improves the glucose conversion which reaches the value of 71 mol% only after 3h, instead of 53 mol% after 6h at 150°C. Moreover, after 1h of reaction at 180°C, the selectivity to fructose is lower than that achieved at 150°C because this last compound has been converted through dehydration giving HMF and the latter has been involved in hydrolysis reaction with the formation of LA and FA which resulted the main products after 6h of reaction. In this case, the LA yield of 24.0 mol% is obtained after 6h, highlighting ZrPO as a promising system for the production of LA at the reaction temperature of 180°C. The increase of kinetics with the rise of temperature is also confirmed by the HMF production: at 180°C the highest HMF yield equal to 17.8 mol% is achieved after 2h of reaction, whereas an analogous value was obtained after 6h at 150°C. The ascertained highest LA yield with ZrPO is better than that reported in the literature by Weingarten et al. where the ZrPO synthesized according to the same procedure with the P/Zr molar ratio of 2 resulted the best system, achieving the highest LA yield of 14.0 mol% working at 160°C [32].~~

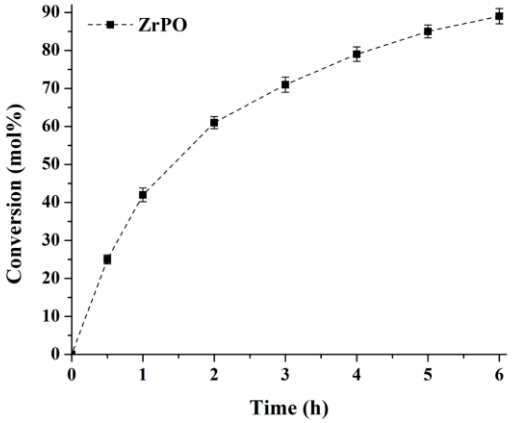
ZrPO
Conversion (mol%)
Time (h)

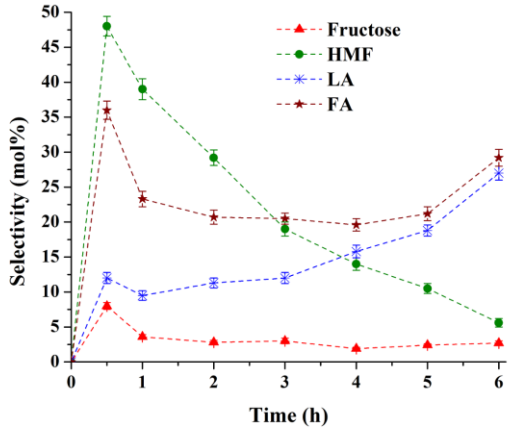
Fructose
HMF
LA
FA
Selectivity (mol%)
Time (h)

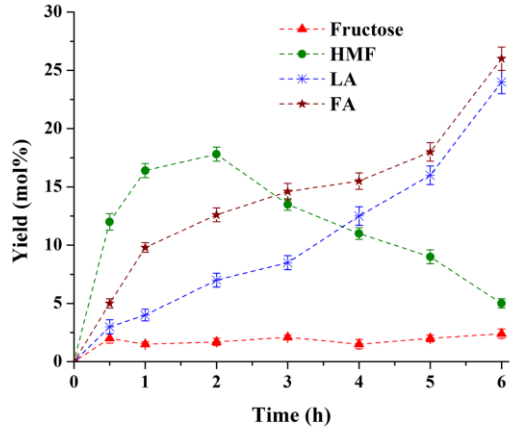
Fructose
HMF
LA
FA
Yield (mol%)
Time (h)

367

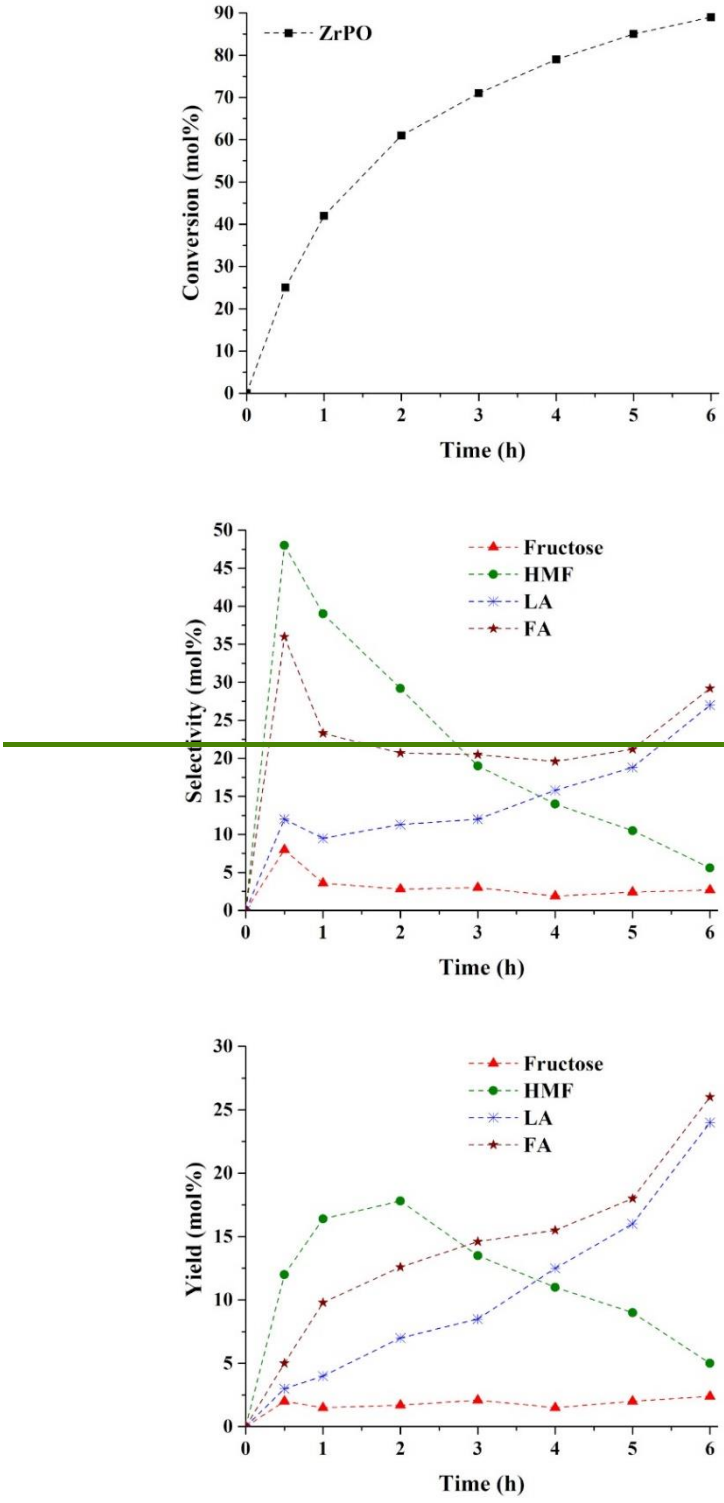

Figure 2: Glucose conversion in the presence of ZrPO as acid catalysts in autoclave at 180 °C. Reaction conditions: glucose = 2.49 g; catalyst = 2.02 g; water = 47.0 g; T = 180 °C. (Note: where the error bars are not visible, they are smaller than the symbols).

The increase of temperature improves the glucose conversion, which reaches the value of 71 mol% ~~only~~ after only 3 h, instead of 53 mol% after 6 h at 150 °C. Moreover, after 1 h of reaction at 180 °C, the selectivity to fructose is lower than that achieved at 150

°C because this last compound has been converted through dehydration ~~giving~~to HMF and the latter has been involved in hydrolysis reaction with the formation of LA and FA which resulted the main products after 6 h of reaction. In this case, the LA yield of 24.0 mol% is obtained after 6 h, highlighting that ZrPO ~~as~~is a promising system for the production of LA at the reaction temperature of 180 °C. The increase of kinetics with the rise of temperature is also confirmed by the HMF production: at 180 °C the highest HMF yield equal to 17.8 mol% is achieved after 2 h of reaction, whereas an analogous value was obtained after 6 h at 150 °C. The ascertained highest LA yield with ZrPO is better than that reported in the literature by Weingarten et al. where the ZrPO synthesized according to the same procedure with the P/Zr molar ratio of 2 resulted the best system, achieving the highest LA yield of 14.0 mol% working at 160 °C [14~~25~~32].

To further improve the selective conversion of glucose towards HMF or LA catalyzed by~~over~~ NbPO and $ZrPO_4$, respectively, several tests have been performed under ~~micro-wave~~MW ~~-~~ irradiation~~,~~. This is~~which is~~ an effective and sustainable tool at the laboratory scale for rapid initial screening, enabling a higher heating rate than traditional heating systems, homogeneous heat distribution, efficient control and remarkable energy- and ~~time~~ time-saving [6~~14~~9]. Firstly, in order to optimize the HMF production with NbPO, the effect of the temperature and reaction time was considered and ~~optimised~~optimized, adopting the same glucose/NbPO weight ratio of 1.2 and the glucose loading of 5 wt%. The obtained results are reported in Table 3~~2~~.

Table 3~~2~~: MW-assisted conversion of glucose carried out in the presence of NbPO catalyst. Reaction conditions: glucose = 0.24 g; catalyst = 0.20 g; water = 4.6 g.

Run	T (°C)	t (min.)	Glucose Conversion (mol%)	Fructose Yield (mol%)	HMF Yield (mol%)	LA Yield (mol%)	HMF Sel. (mol%)	%C recovered (mol%)
1	140	30	40.0	4.3	13.0	1.0	32.5	78.3
2	150	30	36.0	4.6	11.7	0.6	32.5	80.9
3	160	30	54.0	4.0	23.0	1.1	42.6	74.1
4	160	45	64.0	4.0	21.0	4.6	32.8	65.6
5[a]	160	30	29.0	2.0	2.4	-	8.3	75.4
6	170	30	63.0	4.8	19.7	4.6	31.3	66.1
7	180	30	95.0	3.0	19.0	9.0	20.0	36.0

[a] blank test carried out in the absence of catalyst.

Preliminary tests performed at low temperatures (100-120 °C, not shown) led mainly to low amounts of isomerization products (fructose) and up to 5 mol% of HMF yield. This result, although modest in terms of ~~product~~ yield, is related to the presence of strong Lewis acid sites on $NbPO_4$ that catalyze glucose isomerization in aqueous environment at such low temperatures. A further increase of temperature up to 140 °C results in 13 mol% HMF yield and only 1 mol% LA after 30 min of reaction (run 1, Table 3~~2~~). Then, higher temperatures (up to 160 °C) allow improving HMF yields up to 23.0 mol% (runs 2 and 3, Table 3~~2~~), whereas LA yields reach only 1.1 mol%. At 150 °C, after the same reaction time of 30 minutes, in the absence of ~~microwaves~~ MW (Figure 1), both ~~the~~ glucose conversion and ~~the~~ HMF yield resulted lower (glucose conversion 11.9 mol% and HMF yield 7.4 mol% respectively), evidencing ~~microwaves~~ MW as an efficient tool to speed up the

reaction [30~~58~~~~65~~]. Taking into account that the best HMF yield (23.0 mol%) has been achieved working at 160 °C and 30 minutes of reaction (run 3, Table 3~~2~~), a new hydrolysis test was carried out at the same reaction temperature, but for a longer reaction time, equal to 45 minutes (run 4, Table 3~~2~~).~~,~~ In this case, an ~~achieving the~~ almost comparable HMF yield ~~of~~ (21.0 mol%) has been obtained but, due to the subsequent rehydration of HMF to LA (yield of 4.6 mol%), a lower HMF selectivity was ascertained (32.8 mol%).~~, with the corresponding HMF selectivity of 32.8 mol%, due to the subsequent HMF rehydration to LA, whose yield reaches 4.6 mol%.~~ Under the best reaction conditions (run 3, Table 3~~1~~), also a blank experiment was carried out (run 5, Table 3~~2~~), which unequivocally confirmed the key role of the NbPO catalyst for the HMF synthesis. Lastly, higher temperatures were tested (runs 6 and 7, Table 3~~2~~), showing that these are not appropriate for the HMF synthesis, but rather promoting the consecutive formation of LA (run 7, Table 3~~2~~). Adopting MW-irradiation, it is interesting to note that the highest HMF yield (23.0 mol%), which is comparable to that obtained working in autoclave and higher than those reported in the literature for analogous aqueous systems [1,23,24,29~~35~~~~42~~,37~~44~~,44~~51~~], has been reached after only 30 minutes, highlighting again the efficiency of the MW heating. After having identified the optimal temperature for the HMF synthesis (160 °C) adopting ~~microwave~~ MW irradiation, a more thorough investigation of the kinetics was performed, adopting the same glucose/NbPO weight ratio of 1.2 and the glucose loading of 5 wt%, and the corresponding results are shown in Figure 3.

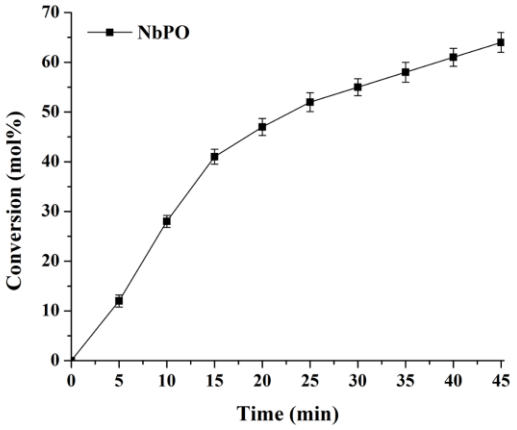
NbPO
Conversion (mol%)
Time (min)

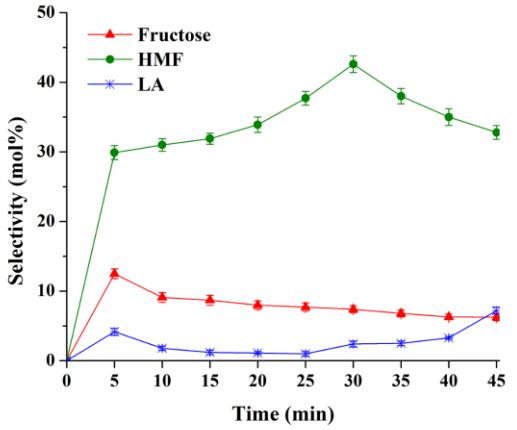
Fructose
HMF
LA
Selectivity (mol%)
Time (min)

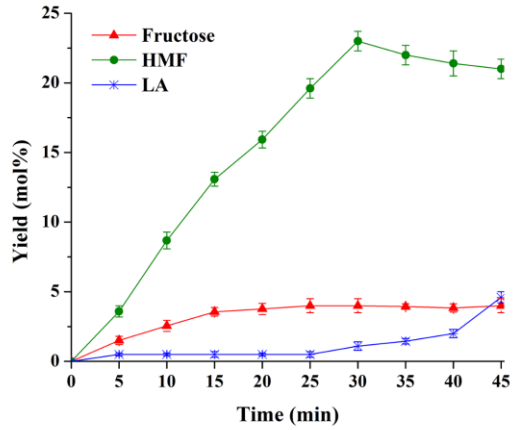
Fructose
HMF
LA
Yield (mol%)
Time (min)

435

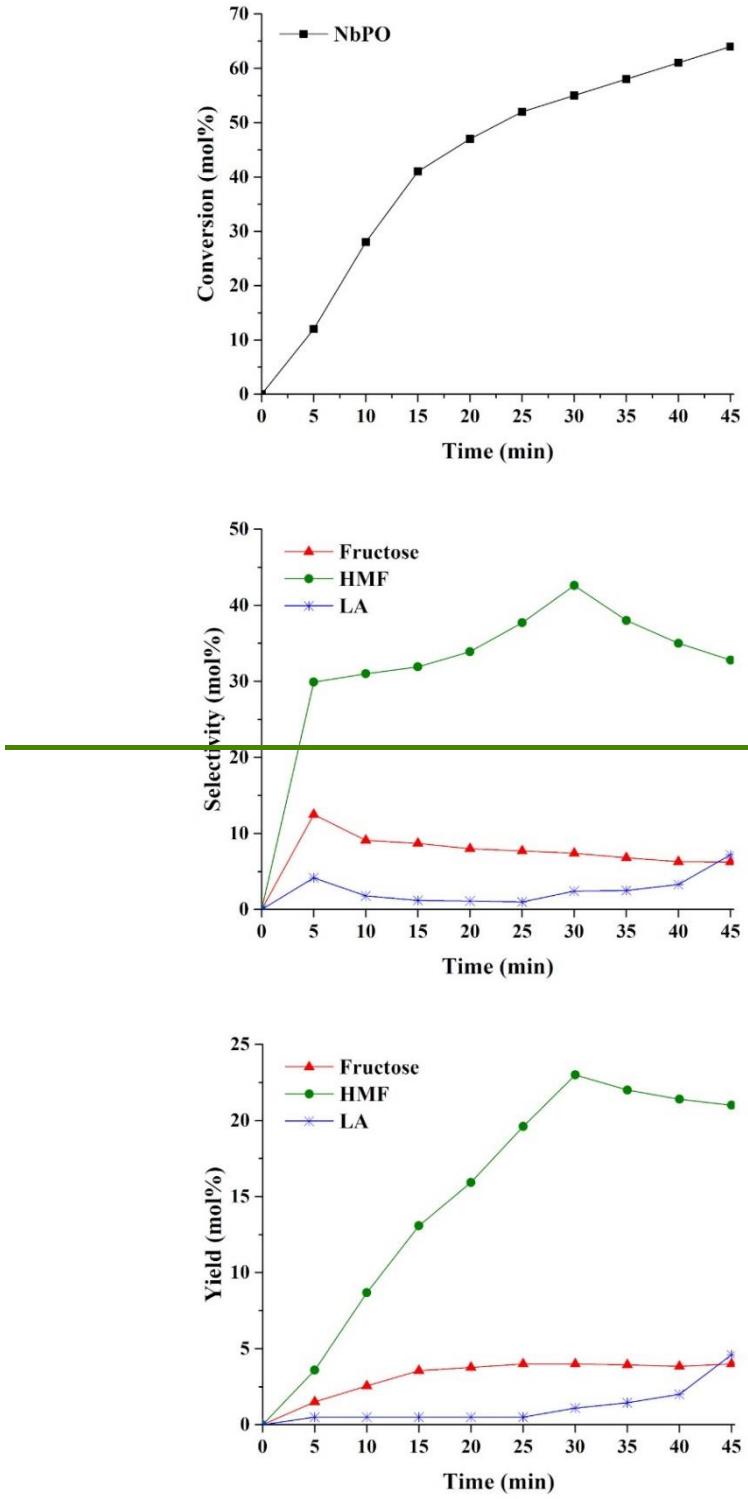

Figure 3: MW-assisted conversion of glucose in the presence of NbPO as acid catalyst at 160 °C. Reaction conditions: glucose = 0.25 g; catalyst = 0.21 g; water = 4.8 g, T = 160 °C. (Note: where the error bars are not visible, they are smaller than the symbols).

Figure 3 shows that the highest HMF yield was obtained working at 160 °C after 30 minutes of reaction, confirming the data already reported in Table 3~~2~~ (run 3). The

selectivity to HMF increases up to 30 minutes of reaction when reaches the maximum value equal to 42.6 mol%, then it slowly decreases, as a consequence of the relevant rehydration of HMF to LA with the simultaneous increase of LA selectivity and yield. Starting from the best MW-assisted hydrolysis test to HMF with NbPO catalyst, also ZrPO was tested under the same reaction conditions (T=160 °C, glucose/ZrPO weight ratio=1.2, glucose loading=5 wt%, t=30 min.). The obtained data with the two catalytic systems are compared in Table 43.

Table 43: MW-assisted conversion of glucose carried out in the presence of ZrPO catalyst. The corresponding hydrolysis experiment with NbPO has been reported for comparison. Reaction conditions: glucose = 0.26 g; catalyst = 0.22 g; water = 5.0 g; T = 160 °C; t = 30 min.

Catalyst	Conversion (mol%)	Fructose Sel. (mol%)	Fructose Yield (mol%)	HMF Sel. (mol%)	HMF Yield (mol%)	LA Sel. (mol%)	LA Yield (mol%)
NbPO	54.0	7.4	4.0	42.6	23.0	2.0	1.1
ZrPO	41.4	4.8	2.0	23.6	9.8	4.4	1.8

TaTable 43 highlights that NbPO shows better catalytic performances in term of conversion, yield and selectivity to HMF than ZrPO, behaviourbehavior in agreement with the corresponding autoclave tests (Figure 1). On this basis, taking into consideration that ZrPO was active for the production of LA at longer reaction time, in order to fully exploit the ZrPO catalyst for the selective synthesis of LA from glucose, new hydrolysis experiments were carried out under microwave MW irradiation, increasing the reaction temperature up to 190 °C and reaction time up to 45 minutes. The results of the MW-assisted experiments are reported in Table 54.

Table 54: MW-assisted conversion of glucose in the presence of ZrPO catalyst at 180 and 190 °C. Reaction conditions: glucose = 0.25 g; catalyst = 0.20 g; water = 4.8 g; t = 45 min.

T (°C)	Conversion (mol%)	Fructose Sel. (mol%)	Fructose Yield (mol%)	HMF Sel. (mol%)	HMF Yield (mol%)	LA Sel. (mol%)	LA Yield (mol%)
160	49.1	6.1	3.0	36.7	18.0	8.9	4.4
180	54.7	5.6	3.1	32.6	17.8	20.8	11.4
190	72.3	2.4	1.7	23.4	16.9	21.9	15.8

The above data are in agreementagree with those reported in the literature regarding the effect of temperature for the LA synthesis [6812,914,149], whose yield increased from 4.4 to 15.8 mol% from 160 to 190 °C after 45 minutes.

In summary, starting from glucose, it is possible to highlight that the different acid properties of the two systems NbPO and ZrPO have enabled us to obtain respectively HMF and LA with maximum yields of 24.4 and 24.0 mol%, respectively, (Figures 1 and 2). These values are higher or comparable with those reported in the literature for analogous systems in aqueous phase [1,14,23,24,292532,3542,3744,4451]. This is an interesting result because it opens the way to study more complex model substrates, such as untreated cellulose, once having verified the stability and recyclability of the catalysts of interest.

2.2 Catalysts sStability and recyclability

Since the stability and the recyclability of the catalysts are of great importance in an applicative and industrial perspective, NbPO and ZrPO were investigated under these aspects. The NbPO and ZrPO catalysts obtained from the best runs to HMF and LA, respectively (run in Figure 1 for NbPO after 6 h and run in Figure 2 for ZrPO after 6 h) were recovered by filtration, washed with acetone and reused within two successive runs performed under the same experimental conditions of the first cycle. The results are reported in Table 65.

Table 65: Glucose conversion in the presence of NbPO (T = 160 °C) and ZrPO (T = 180 °C) under the same reaction conditions (6 h, glucose/catalyst weight ratio = 1.2, glucose loading = 5 wt%) and two subsequent recycles of the solid catalysts.

	Glucose conversion (mol%)	HMF Selectivity (mol%)	HMF Yield (mol%)
Fresh NbPO	78.6	31.0	24.4
NbPO used first cycle	76.9	30.2	23.2
NbPO used second cycle	75.5	30.1	22.7
	Glucose conversion (mol%)	**LA Selectivity (mol%)**	**LA Yield (mol%)**
Fresh ZrPO	89.0	27.0	24.0
ZrPO used first cycle	88.6	27.0	23.9
ZrPO used second cycle	86.3	26.6	23.0

The obtained results confirm the feasibility of catalyst reactivation by simple acetone washing, showing, for both phosphates, only a slight decrease in glucose conversion and HMF/LA ~~selectivity~~ selectivities and yields. The good efficiency of the washing ~~method~~ suggests that ~~the~~ most of the furanic polymers adsorbed on the catalysts surface, probably deriving from condensation reactions, are soluble ones~~, thus easily removable by acetone~~.

In order to verify the presence of organic deposits on spent catalysts, FT-IR analyses of NbPO and ZrPO recovered at the end of the best reactions were compared with those of fresh and washed samples. The recorded spectra are shown in Figure 4.

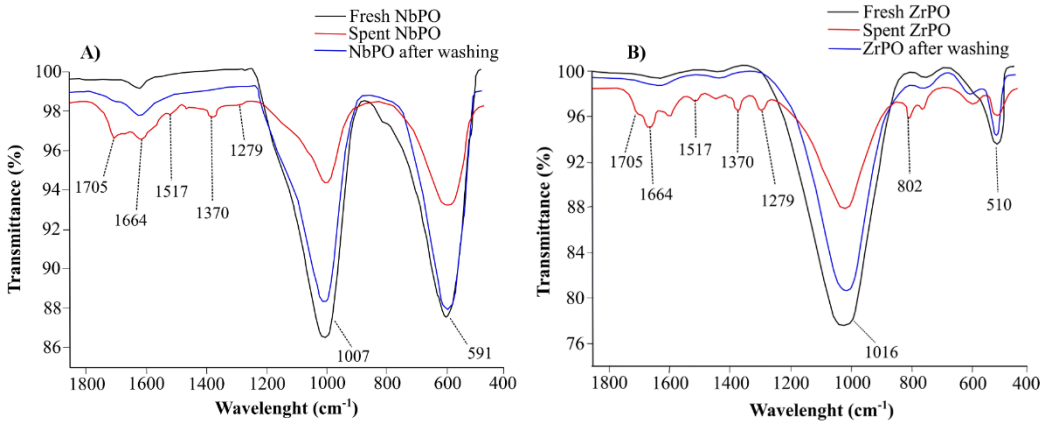

Figure 4: Comparison between FT-IR spectra of fresh NbPO and ZrPO catalysts, spent catalysts and catalysts after washing reactivation in wavenumber range of 1850-430 cm^{-1}: A) NbPO and B) ZrPO.

The spectra of the spent catalysts show characteristic bands of soluble or insoluble humins, proving the deposition of organic compounds on the catalysts surface. In fact, absorption bands at 1705 cm^{-1}, 1517 cm^{-1}, 1370 cm^{-1} and 1279 cm^{-1} can be identified both in spent NbPO and ZrPO spectra, assigned respectively to stretching of C=O of carbonyl groups, stretching of C=C in furan and/or aromatic compounds, stretching of C-O-C bond of furan ring and stretching of C-O bond of ethers [236]. In addition, the spectra of the spent NbPO and ZrPO catalysts shows another band at 1664 cm^{-1}, due to stretching of C=O of quinones., Moreover, whereas in the spectrum of the spent ZrPO, appears an additional band at 802 cm^{-1} appears, due to bending out of plane of =C-H bond of aromatic and/or furan rings [315966]. In Figure 4, the IR spectra of NbPO and ZrPO after the washing treatment are also reported. It is interesting to highlight that the FT-IR spectra of the catalysts after the acetone washing are very similar to those of the fresh samples, thus confirming the feasibility of this the proposed simple reactivation method, as indirectly suggested by the recycle recycling tests. The moderate formation of humins during the reaction is also confirmed by SEM analyses, which are reported in Figure 5.

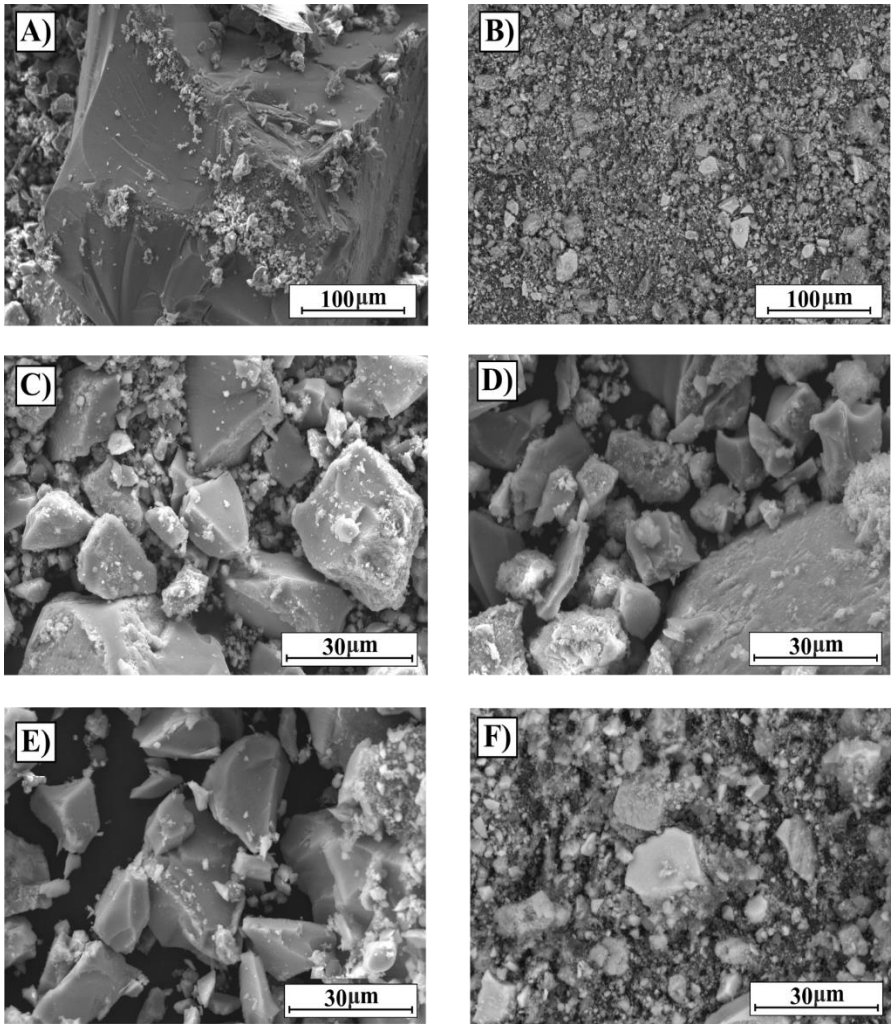

Figure 5: Scanning electron microscopy (SEM): A) fresh NbPO, B) fresh ZrPO, C) spent NbPO, D) spent ZrPO, E) washed NbPO and F) washed ZrPO.

From the SEM of the fresh NbPO and ZrPO, it is possible to see that ~~both catalysts~~ the morphology of both catalysts ~~is formed by~~reveals pieces and surfaces with irregular dimensions ~~and surfaces~~. For the spent catalysts, NbPO and ZrPO employed at 160 and 180 °C respectively (run in Figure 1 after 6 h for NbPO and run in Figure 2 after 6 h for ZrPO), it is possible to observe a few regions covered with particles of spherical morphologies, resulting coalesced with each other. Such particles have similar characteristics to insoluble humic compounds, characterized by Patil and Lund [32607], ~~which confirm s~~confirming the limited formation of these compounds during the reaction. Figure 5 also shows the washed catalysts, which appear similar to fresh ones, again confirming the feasibility of the washing procedure.

This is also evidenced by TGA analyses on fresh, spent and washed NbPO and ZrPO. The obatined results are shown in Figure 6 ~~performed and shown in Figure 6~~.

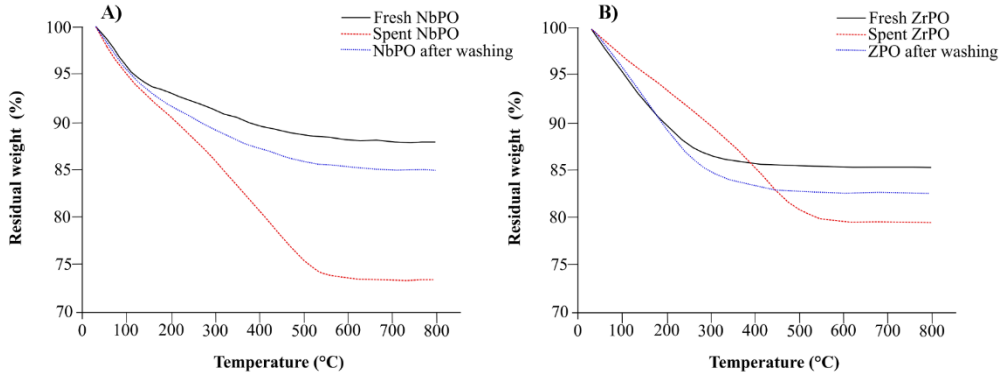

Figure 6: TGA analysis: A) fresh, spent and washed NbPO, B) fresh, spent and washed ZrPO.

The weight loss observed between 30 and 200 °C was due to water and ~~other possible~~ volatile organic compounds (VOCs) [3368] present in the fresh catalysts. At higher temperatures (between 200-500 °C), for the spent NbPO an additional weight loss was observed ~~of~~ (about 17 wt%), due to humins adsorbed on the catalyst surface [33618]. On the other hand, for the spent ZrPO, a lower weight loss ~~of~~ (about 11 wt%) was ascertained between 200-500 °C, thus highlighting a lower amount of adsorbed humins on this catalyst. However, for both catalytic systems, the amount of adsorbed humins is limited and the reactivation treatment performed through acetone washing ~~with acetone~~ allowed their removal and the restore of the starting catalytic activities.

Moreover, EDS analysis of both phosphates was performed estimating that, on the basis of the elements Nb, Zr and P, the fresh NbPO contains 89.5 wt% of niobium and 10.5 wt% of phosphorus, whereas the fresh ZrPO is composed by 60.8 wt% of zirconium and 39.2 wt% of phosphorus. By comparing these results with those of the catalysts after the reactions, it is possible to demonstrate the stability of these phosphates in the adopted reaction conditions: the niobium amount resulted 89.9 wt% in the spent NbPO system, with phosphorus amount equal to 10.1 wt%, whereas for spent ZrPO system the zirconium amount was 61.4 wt% with 38.6 wt% of phosphorus amount. These results are in agreement with XRF analyses~~,~~ that showed ~~from which~~ for the fresh systems the molar ratio P/Zr and P/Nb resulted 1.90 ± 0.1 and 0.33 ± 0.05 respectively ~~,~~ On this basis, its is possible to undoubtedly confirm ~~undoubtedly confirming~~ the negligible leaching of Nb and Zr in the aqueous phase under the adopted reaction conditions. This last aspect was also verified comparing the best catalytic results achieved in the presence of the catalysts (run in Figure 1 for NbPO after 6 h and run in Figure 2 after 6 h for ZrPO) with those obtained after the removal of the catalysts from ~~in~~ the reaction medium. For NbPO, after 6 h, the glucose conversion slightly increased, moving from 78.6 to 80.3 mol%, with an almost comparable HMF yield (24.5 mol%). For ZrPO, after 6 h, the same trend was

observed, increasing the glucose conversion from 89.0 to 89.9 mol%, together with a similar HMF yield (24.3 mol%).

Finally, ~~the porosity~~ porosities and texture properties of the fresh and spent NbPO and ZrPO systems were analyzed using nitrogen physisorption isotherms, as reported in Figure 7 and Table ~~6~~7. All samples show type IV isotherms, typical of mesoporous materials [34~~6~~29]. In the case of NbPO samples, very low amount of microporosity is also present. Noteworthy, both Zr and Nb spent catalysts show an increase of the hysteresis, due to the formation of ink-bottle pores with the neck size smaller than the average diameter or in general due to the presence of pores with diverging radius along their length. This could be ascribable to the deposition of carbonaceous residue inside the porosities probably with a greater extent on the external part of the pores. Nonetheless, while NbPO shows a marked decline in both SSA and pore volume suggesting the occlusion of some of the pores (narrower compared to the ones of ZrPO, 9 nm compared to 16 nm) this is not the case for ZrPO, in agreement with the observed catalytic performances and TGA analyses.

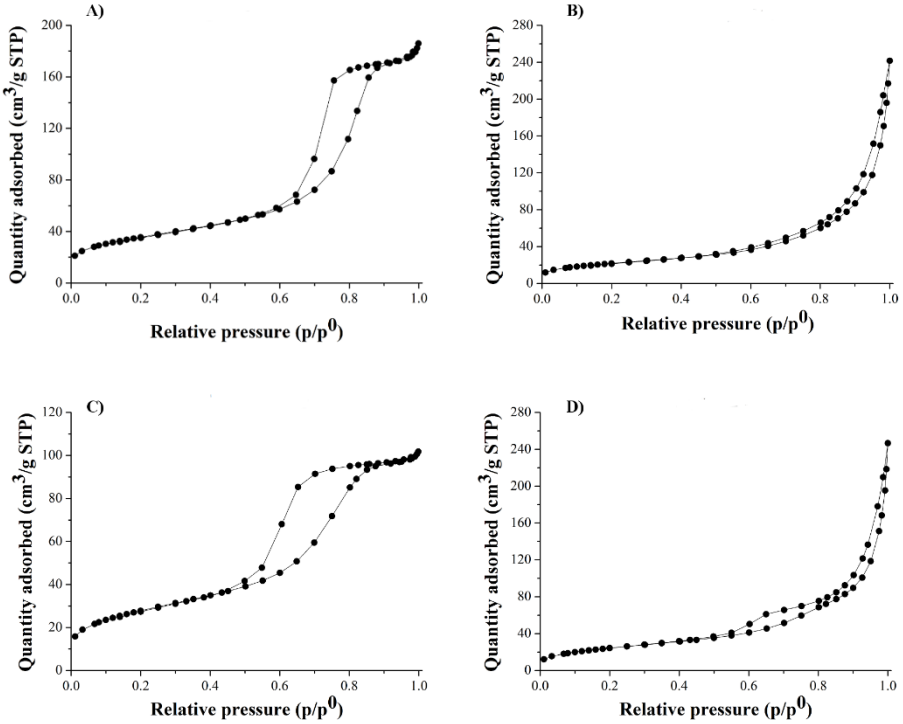

Figure 7: N_2 adsorption and desorption isotherms: A) fresh NbPO, B) fresh ZrPO, C) spent NbPO, D) spent ZrPO.

Table ~~7~~6: Texture properties of catalysts: a) fresh NbPO, b) spent NbPO, c) fresh ZrPO, d) spent ZrPO.

Sample	Surface Area (m^2/g)	Total Pore Volume (cm^3/g)	Micropore Volume (cm^3/g)	Micropore Area (m^2/g)	Average Pore Diameter (nm)
Fresh NbPO	133	0.28	0.004	13	9
Fresh ZrPO	108	0.33	0	2	16
Spent NbPO	101	0.16	0.001	6	6
Spent ZrPO	90	0.33	0	0	14

In conclusion, NbPO and ZrPO are characterized by a high stability and an easy recyclability, making these systems promising for their use also with more complex substrates.

2.3~~2~~ Conversion of untreated cellulose in the presence of NbPO and ZrPO

After the catalytic tests with glucose ~~as starting feedstock~~, the reactivity of the more recalcitrant microcrystalline cellulose was studied in autoclave. ~~–~~Starting from the reaction conditions optimized in a previous work on the conversion of cellulose ~~and new catalytic runs were carried out starting from the reaction conditions optimized in a previous work for cellulose itself~~ [35637~~0~~], new catalytic runs were carried out at ~~working at the same temperature of~~ 150 °C, as in the conversion of glucose in autoclave, ~~as in the study of glucose for the autoclave reactions~~ and under autogenic pressure, with the same substrate/catalyst weight ratio of 1.2 and cellulose loading of 5 wt%, ~~monitoring~~ prolonging the reaction up ~~the reaction up~~ to 24 hours. The obtained results are reported in Figure 8.

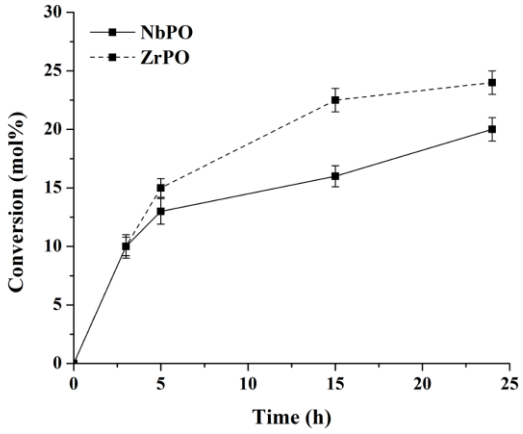
NbPO
ZrPO
Conversion (mol%)
Time (h)

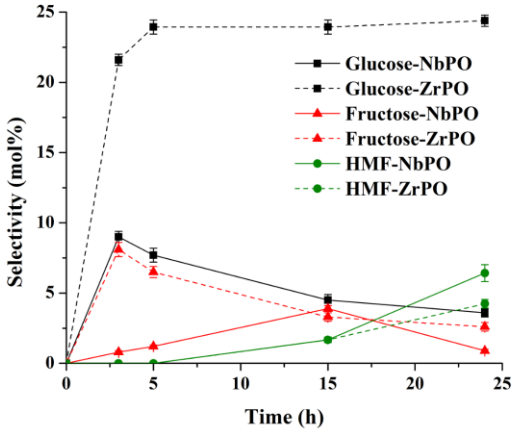
Glucose-NbPO
Glucose-ZrPO
Fructose-NbPO
Fructose-ZrPO
HMF-NbPO
HMF-ZrPO
Selectivity (mol%)
Time (h)

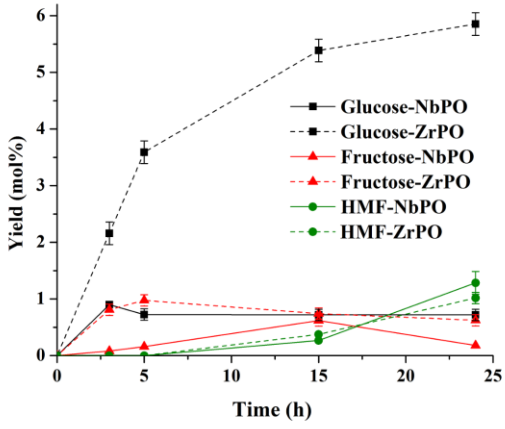
Glucose-NbPO
Glucose-ZrPO
Fructose-NbPO
Fructose-ZrPO
HMF-NbPO
HMF-ZrPO
Yield (mol%)
Time (h)

621

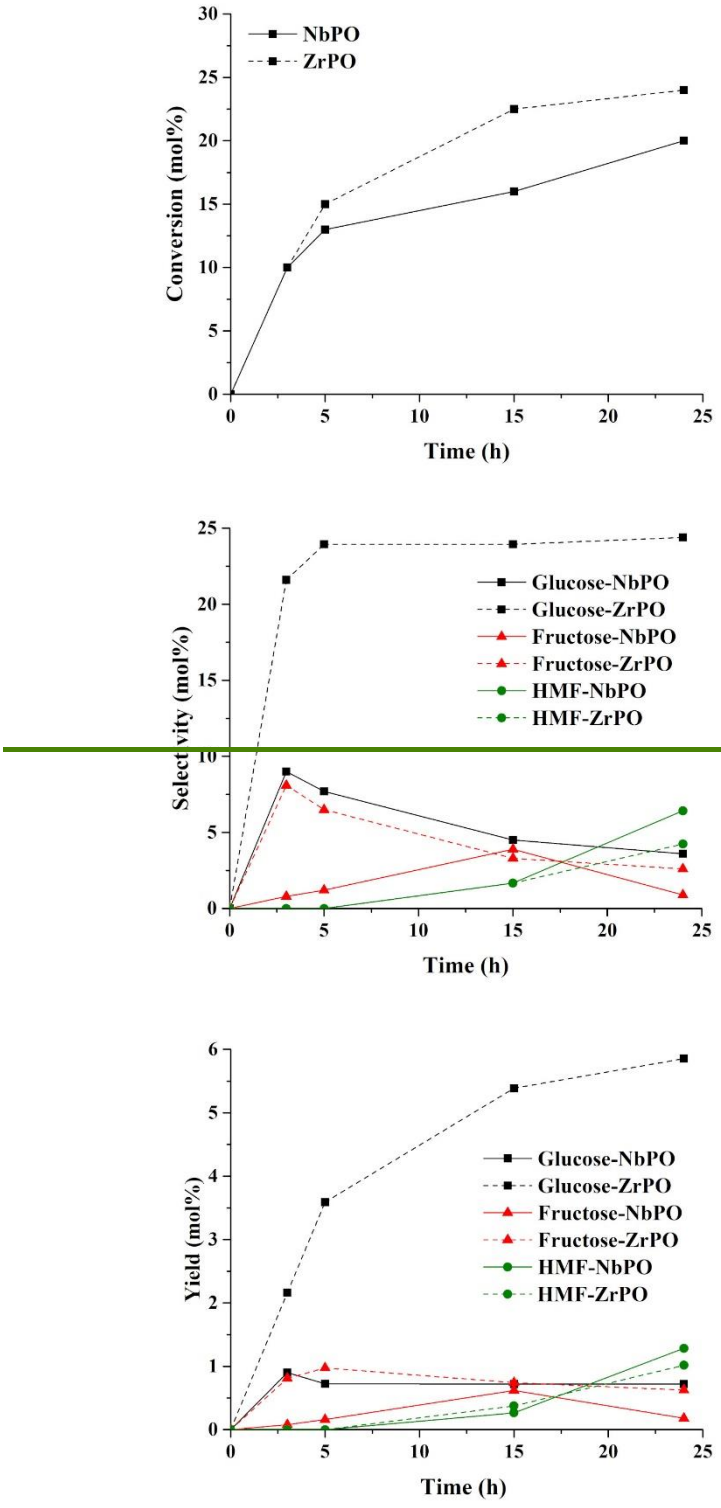

Figure 8: Catalytic performances of NbPO and ZrPO in the conversion of untreated cellulose at 150 °C. Reaction conditions: cellulose = 2.63 g, catalysts = 2.20 g, water = 50.0 g, T = 150 °C, autogenic pressure (LA is present only in traces). (Note: where the error bars are not visible, they are smaller than the symbols).

In addition to the reported catalytic runs, blank test for the conversion of untreated cellulose at 150 °C and 24 h has been performed, obtaining the cellulose conversion of 7 mol%, the glucose yield of 2.3 mol% and only traces of HMF and LA. As it is possible to appreciate from Figure 8, for both catalytic systems, the cellulose conversion is low, about 20-25 mol%, even if higher to that achieved in the blank experiment, with the highest glucose yield of about 6 mol% reached with ZrPO, value comparable with that reported in the literature adopting ZrPO under analogous reaction conditions (glucose yield 5.8 wt% equal to 5.2 mol%) [3563~~70~~]. It is interesting to note that, starting from cellulose, the higher conversion is achieved with ZrPO, instead of NbPO as in the case of glucose. This behaviour can be justified taking into consideration that starting from cellulose its preliminary hydrolysis step to glucose is necessary~~the additional preliminary hydrolysis step of this compound to glucose is necessary~~ and this reaction is mainly catalyzed by Brønsted acidity~~,~~ but also by Lewis acid sites. In fact, it is known that for an efficient cellulose hydrolysis, solid acids must be able to adsorb β-1,4-glucans on the surface and interact with them by means of, for example, acid -OH groups.~~,~~ This interaction can be also promoted by Lewis acid sites [3664] and allows the decrease of activation energy of the hydrolysis step. ~~that decrease the activation energy for the hydrolysis reaction and this interaction can be also promoted by the presence of surface Lewis acid sites~~ [~~71~~]. On this basis, adopting the same amount of NbPO and ZrPO, the ascertained conversion behavio~~u~~r is in agreement with their total acidity, which is higher for ZrPO than NbPO. Regarding the products distribution, ZrPO shows a higher selectivity towards glucose than NbPO and this can be justified by the higher amount of total acid sites and the lower Brønsted/Lewis molar ratio of ZrPO, which are respectively responsible for the faster hydrolysis of cellulose to glucose and the slower glucose conversion compared to NbPO, as previously found. At the same time, the lower Brønsted/Lewis molar ratio of ZrPO than NbPO justifies the higher fructose selectivity observed for ZrPO than NbPO. On the other hand, NbPO results more selective towards HMF than ZrPO, in particular at long reaction time, due to NbPO balanced Brønsted and Lewis acid properties. However, the selectivities of the target products are low for both catalysts (also LA is present only in traces) in the whole investigated time range, suggesting the presence of other not quantified products, such as oligomers, whose formation is promoted rather than that of glucose, due to the limited heterogeneous catalyst interaction with the solid substrate, that hampers the hydrolysis step. However, the possibility to obtain hydrolysates rich in ~~cellulose~~ cellulose-derived oligomers is very interesting, because these are produced under heterogenous catalysis, avoiding any contamination by mineral acids, generally employed for their production. Such hydrolysates can be valorized in a plethora of compounds by subsequent catalytic and/or biocatalytic conversion cascade processes, once separated the solid fraction.

It is well known that cellulose is more recalcitrant than glucose towards hydrolysis due to its stable H-bonds networks and high crystalline structure~~The low conversion achieved with this more complex substrate is also due to the higher recalcitrance of the cellulose with respect to glucose, caused by its high crystalline structure and its stable H-bonds networks~~, as confirmed by its XRD analysis ~~reported in~~ (Figure 9), where the main peak at 2θ=22.5° is attributed to the crystalline fraction. This justifies the lower conversion achieved starting from cellulose.

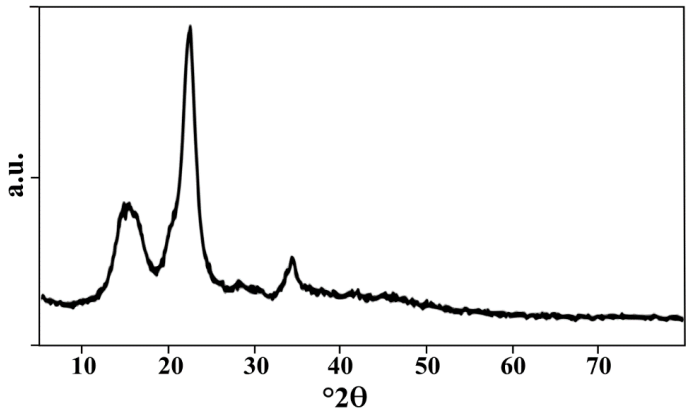

Figure 9: XRD analyses of microcrystalline cellulose.

2.~~3~~ Hydrolysis of real lignocellulosic biomasses

On the basis of the promising catalytic performances achieved with NbPO and ZrPO on model compounds, these systems were also employed with real lignocellulosic biomasses, to confirm the correlation between physical-chemical properties of NbPO and ZrPO and their performances, previously identified from the study of model compounds. Conifer wood sawdust was firstly considered as the reference biomass for the hydrolysis tests. Its composition, in terms of cellulose, hemicellulose and lignin, is equal to 45, 20 and 30 wt% respectively, with 5 wt% of others (extractives, resins and ash). Hydrothermal conversion of conifer wood sawdust into sugars and dehydration/hydrolysis products was investigated in the autoclave, first without any catalyst, and then in the presence of NbPO and ZrPO catalytic systems, working at 150 °C with the same substrate/catalysts weight ratio of 1.2 and the biomass loading of 5 wt%. In the absence of catalyst, the hemicellulose conifer wood sawdust conversion was complete, whereas the conversion of its cellulose fraction amounted to 7.6 mol%. In addition, the yield to total monosaccharides from hemicellulose resulted equal to 10.6 mol%, together with traces of monosaccharides from cellulose. In the presence of NbPO and ZrPO the results are shown in Figure 10.

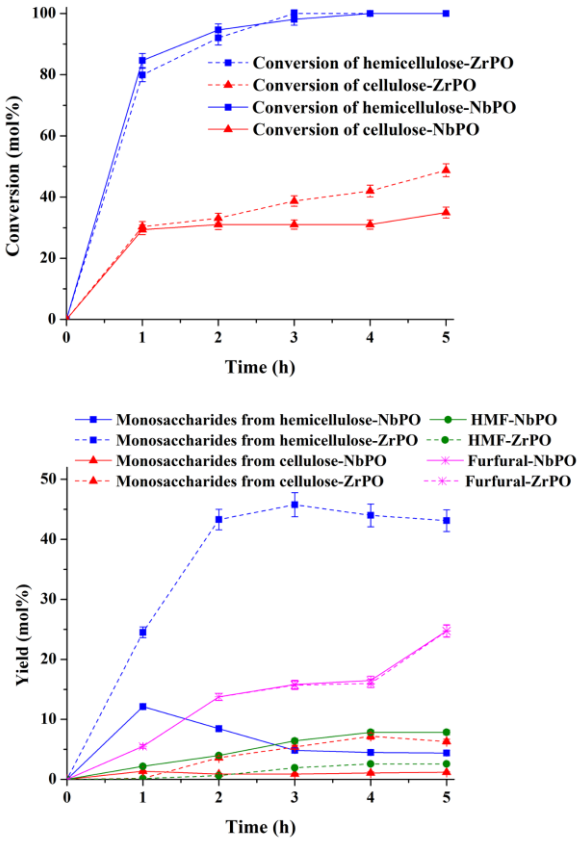

Figure 10: Catalytic performances of NbPO and ZrPO in the conversion of conifer wood sawdust at 150 °C. Reaction conditions: biomass = 2.68 g catalysts = 2.23 g water = 51.0 g T = 150 °C, autogenic pressure. As reported in the Materials and Methods, yields have been calculated with respect to the amount of cellulose or hemicellulose present in the starting biomass. (Note: where the error bars are not visible, they are smaller than the symbols).

Noteworthy, for both metal phosphates, the conversion of hemicellulose fraction of lignocellulosic substrate is very fast, resulting almost complete for both systems after 3 h. On the other hand, the conversion of cellulose fraction is slower, reaching values of 34.9 and 48.8 mol% after 5 h for NbPO and ZrPO, respectively. The observed behaviour is expected: hemicellulose hydrolysis proceeds faster and smoother than that of cellulose ~~if compared to the conversion of cellulose~~, as proved by the higher yields to monosaccharides deriving from hemicellulose (xylose, arabinose, galactose and mannose) reached adopting both phosphates. These sugars yields reached the maximum value at medium-low reaction time, respectively 45.8 mol% after 3 h for ZrPO and 12.1 mol% after 1 h for NbPO; then, in both ~~the~~ cases, these yields decreased due to the increase of decomposition products. Again, Zr-based catalyst shows higher yield and selectivity towards hemicellulose and cellulose sugars compared to the Nb analogue, while the latter leads to higher yield and selectivity towards HMF. This behaviour is in good agreement with that observed with glucose and cellulose. ZrPO is more active ~~in~~ to the degradation of both cellulose and hemicellulose fractions, as shown by the higher achieved cellulose conversion ~~achieved~~, the most recalcitrant fraction~~, with this catalyst compared to NbPO~~. Conversely, NbPO mainly promotes the formation of furanic derivatives. In fact, the decrease of monosaccharides yield for NbPO begins after only 1 h of reaction time, especially for those deriving from the hemicellulose fraction, that is a much shorter reaction time compared to the 3 h needed with ZrPO. Therefore, it is possible to confirm the effects already found for the hydrolysis of cellulose: the higher total concentration of acid sites, shown

by ZrPO, results in a higher activity in lignocellulose conversion and consequently in a higher production of monosaccharides from both hemicellulose and cellulose hydrolysis. On the other hand, the higher amount of strong Brønsted acid sites, exhibited especially in aqueous conditions~~, exhibited~~ by NbPO, mainly promotes the dehydration of monosaccharides, deriving from both cellulose and hemicellulose fractions, to the successive furan products, such as HMF and furfural. The achieved results are comparable with those reported in the literature by Gliozzi et al. who studied the conversion of conifer wood sawdust in the presence of different acid catalysts [35~~63~~70]. In fact, in the presence of ZrPO, after 5 h of reaction, the authors ascertained at 150 °C the biomass weight conversion of 41 wt%, equal to 41.9 wt% achieved in the present work (100 mol% of hemicellulose fraction + 48.7 mol% of cellulose fraction), together with the yield to hemicellulose derived sugars of 49.2 mol% and yield to cellulose derived sugars of 3.4 mol%, perfectly in ~~line~~ agreement with the values ascertained here, 43.1 and 6.3 mol% from hemicellulose and cellulose fractions, respectively.

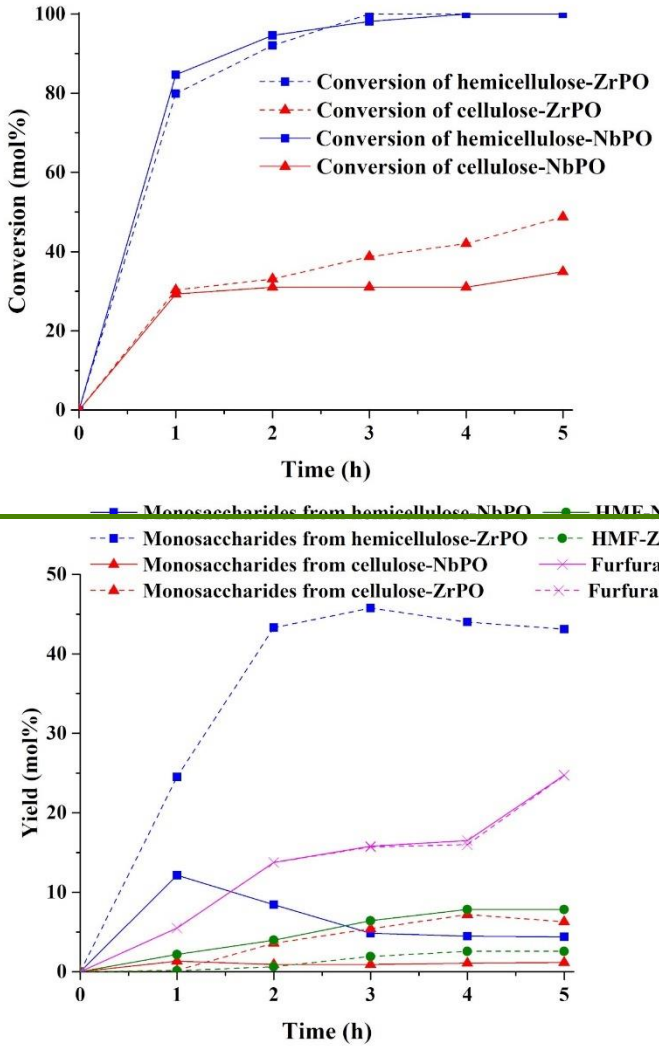

Figure 10: Catalytic performances of NbPO and ZrPO in the conversion of conifer wood sawdust at 150°C. Reaction conditions: biomass = 2.68 g catalysts = 2.23 g water = 51 g T = 150 °C, autogenic pressure. As reported in the Materials and Methods, yields have been calculated with respect to the amount of cellulose or hemicellulose present in the starting biomass.

After having established that the catalytic behaviour of Nb and Zr phosphates in hydrolysis reaction is closely related to the catalysts acid properties also in the case of the reference lignocellulosic substrate (conifer wood sawdust), the conversion of a wider range of six real lignocellulosic biomasses was investigated. In particular, Jerusalem artichoke, sorghum, miscanthus, foxtail millet, hemp and *Arundo donax* whose starting compositions are reported in Table 87, were tested at 150 °C for 1 h in the presence of both Nb and Zr phosphates, adopting the same catalyst/substrate weight ratio of 1.2 and the starting biomass loading of 5 wt%. The results are shown in Tables 98 and 109.

Table 87: Average compositions of the lignocellulosic biomasses employed in the present work.

Biomass	Cellulose (wt%)	Hemicellulose (wt%)	Lignin (wt%)	Others (wt%)
Jerusalem artichoke	16.0	7.5	6.1	70.4
Sorghum	35.7	27.8	6.5	30.0
Miscanthus	23.8	30.9	13.4	31.9
Foxtail millet	16.0	30.9	22.9	30.2
Hemp	62.6	15.1	7.4	14.9
Arundo donax	36.3	24.6	9.4	29.7

Table 98: Catalytic performances of NbPO in the conversion of lignocellulosic biomasses at 150 °C. Reaction conditions: biomass = 2.69 g catalysts = 2.24 g water = 51.0 g T = 150 °C, autogenic pressure, 1 h. As reported in the Materials and Methods, yields have been calculated with respect to the amount of cellulose or hemicellulose present in the starting biomass.

Catalyst: NbPO Biomass	Jerusalem artichoke	Sorghum	Miscanthus	Foxtail millet	Hemp	Arundo donax
Biomass cellulose conversion (mol%)	76.4	37.8	61.1	73.9	10.7	34.1
Biomass hemicellulose conversion (mol%)	100.0	66.1	66.2	70.2	97.5	69.9
Yield to cellulose derived sugars (mol%)	19.2	21.9	18.7	24.9	0.6	10.8
Yield to cellulose oligomers (mol%)	23.1	1.7	31.2	29.6	3.1	12.7
Yield to hemicellulose derived sugars (mol%)	18.8	16.6	25.9	31.2	10.8	20.7

Yield to hemicellulose oligomers (mol%)	34.2	35.1	26.3	26.0	32.6	33.1
Yield to HMF (mol%)	8.6	9.4	5.9	11.7	0.3	5.7
Yield to furfural (mol%)	4.1	2.9	3.7	5.6	2.1	2.9
%C recovered (mol%) respect to starting cellulose amount	74.5	95.2	94.7	92.3	93.3	95.1
%C recovered (mol%) respect to starting hemicellulose amount	57.1	88.5	89.7	92.6	48.0	86.8

Table 10~~9~~: Catalytic performances of ZrPO in the conversion of lignocellulosic biomasses at 150 °C. Reaction conditions: biomass = 2.67 g catalysts = 2.22 g water = 51.0 g T = 150 °C, autogenic pressure, 1 h. As reported in the Materials and Methods, yields have been calculated with respect to the amount of cellulose or hemicellulose present in the starting biomass.

Catalyst: ZrPO Biomass	**Jerusalem artichoke**	**Sorghum**	**Miscanthus**	**Foxtail millet**	**Hemp**	**Arundo donax**
Biomass cellulose conversion (mol%)	97.7	49.9	78.2	85.5	14.9	41.4
Biomass hemicellulose conversion (mol%)	100.0	74.2	76.7	76.5	100.0	65.0
Yield to cellulose derived sugars (mol%)	50.0	31.0	25.0	35.5	2.3	14.2
Yield to cellulose oligomers (mol%)	28.4	5.2	48.0	44.9	3.1	21.4

Yield to hemicellulose derived sugars (mol%)	21.0	19.5	24.6	34.7	10.2	20.6
Yield to hemicellulose oligomers (mol%)	34.4	34.6	26.5	26.2	41.3	33.2
Yield to HMF (mol%)	4.5	5.9	3.7	5.1	1.5	2.4
Yield to furfural (mol%)	1.9	1.4	1.5	2.3	2.1	1.9
%C recovered (mol%) respect to starting cellulose amount	85.2	92.2	98.5	100.0	92.0	96.6
%C recovered (mol%) respect to starting hemicellulose amount	57.3	81.3	75.9	86.7	53.6	90.7

The results evidence that the catalytic performances are significantly affected by the composition of the substrates. For both catalysts and for most biomasses (except for foxtail millet with ZrPO), the conversion of hemicellulose is higher or comparable than that of cellulose, and this is in agreement with the easier hydrolysis of the C5 fraction than C6 one. In particular, the percentage of the hardly hydrolyzable cellulose present in the starting biomass ~~, which is harder to be hydrolyzed,~~ compared to hemicellulose amount~~,~~ influences the biomass conversion: in fact, hemp, which is characterized by a cellulose content of 62.6 wt%, shows the lowest cellulose conversion with both phosphates, 10.7 and 14.9 mol% for NbPO and ZrPO, whereas Jerusalem artichoke reveals the highest conversions of cellulose, equal to 76.4 and 97.7 mol% for NbPO and ZrPO, due to the lower cellulose percentage of only 16.0 wt%. Regarding the products yields, the achieved results employing the six agricultural waste substrates are in good accordance with those obtained from glucose and cellulose, but also for the reference biomass conifer wood sawdust: ZrPO shows a higher selectivity towards ~~cellulose~~ cellulose-derived sugars and ~~cellulose~~ cellulose-oligomers compared to NbPO, whereas the behavior towards hemicellulose derived sugars and hemicellulose oligomers is similar for the two catalysts. The possibility of obtaining such hydrolysates~~,~~ rich in hemicellulose- and ~~cellulose~~ cellulose-derived sugars~~/ and~~ oligomers, in particular those prepared ~~especially for those obtained~~ by Jerusalem artichoke, miscanthus and foxtail millet with NbPO and ZrPO, characterized by a high hemicellulose and cellulose solubilization, opens the way to many subsequent catalytic and/or biocatalytic ~~conversion~~ cascade processes towards the production of several compounds.~~a plethora of compounds,~~ Moreover, the employment of heterogeneous catalysts allows avoiding any contamination once separated the solid residue, as instead happens with mineral acids, generally employed for this reaction ~~once separated the solid residue, avoiding any contamination by mineral acids, generally employed for their production~~ [37,38~~65~~72,66~~73~~]. In the perspective of a such cascade process, the recovered solid residue could be exploited by many strategies, according to the sustainability criteria. In fact, the final solid residue is a hydrochar, more similar to lignin than to the starting lignocellulosic biomasses and, as such, it could be used in energy and environmental fields, including the applications as adsorbents, precursor of catalysts, soil amendment, anaerobic digestion, composting and electrochemical energy storage materials [39~~67~~74].

Moreover, as previously stated, NbPO shows a prevailing performance towards sugar consecutive products, such as HMF and furfural, whose yield for NbPO are higher with respect to those observed for ZrPO. Respect to conifer wood sawdust, after 1 h of reaction, Jerusalem artichoke biomass shows a higher cellulose conversion with both phosphates than conifer wood sawdust (97.7 mol% with ZrPO and 76.4 mol% with NbPO

for Jerusalem artichoke respect to 30.3 mol% with ZrPO and 29.3 mol% with NbPO for conifer wood sawdust). The higher conversion achieved for Jerusalem artichoke rather than conifer wood sawdust is also observed for its hemicellulose fraction after 1 h of reaction with both catalysts (100.0 mol% with ZrPO and NbPO for Jerusalem artichoke respect to 79.9 mol% with ZrPO and 84.6 mol% with NbPO for conifer wood sawdust). In addition, also the yields to monosaccharides deriving from cellulose with both phosphates are higher than the corresponding ones achieved with conifer wood sawdust. In fact yields of cellulose derived sugars ~~, employing Jerusalem artichoke after 1 h of reaction yields to cellulose derived sugars~~ equal to 50.0 ~~–~~and 19.2 mol% with ZrPO and NbPO were obtained starting from Jerusalem artichoke, higher than those ascertained from conifer wood sawdust (0.2 and 1.4 mol% with ZrPO and NbPO, respectively)."~~with ZrPO and NbPO respectively were obtained than 0.2 (with ZrPO) and 1.4 (with NbPO) mol% starting from conifer wood sawdust.~~ Regarding yields to ~~hemicellulose~~ hemicellulose-derived sugars, it is possible to underline that after 1 h of reaction in the presence of ZrPO, comparable values were reached with Jerusalem artichoke and conifer wood sawdust (21.0 mol% for Jerusalem artichoke and 24.5 mol% for conifer wood sawdust), whereas under the same reaction conditions in the presence of NbPO a higher yield to hemicellulose derived sugars was obtained starting from Jerusalem artichoke (18.8 mol%) than conifer wood sawdust (12.1 mol%). Moreover, taking into consideration the yield to furanic compounds (HMF + furfural), the achieved yields starting from Jerusalem artichoke are higher than those obtained with conifer wood sawdust (6.4 mol% with ZrPO and 12.7 mol% with NbPO for Jerusalem artichoke respect to 5.6 mol% with ZrPO and 7.7 mol% with NbPO for conifer wood sawdust). The achieved results highlight ~~as~~ that Jerusalem artichoke ~~can be~~is a promising biomass ~~for the production of~~to produce furanic compounds and ~~cellulose~~ cellulose-derived sugars after only 1 h of reaction, in the presence respectively of NbPO and ZrPO.

In the literature, it is rare the use of metal phosphates to produce HMF from real biomasses and the substrates are mostly limited to monosaccharides [1]. In this perspective, ~~starting from waste biomasses,~~ Parshetti et al. investigated the conversion of food waste biomass to HMF, reaching under the best reaction condition the HMF yield of 4.3 w~~teight~~ % in the presence of ZrPO calcinated at 400 °C after 6 h of reaction [28~~48~~55]. ~~,~~ This value is comparable with those reached in the present work ~~value in the same range of those reached by us only~~ after only 1 h of reaction starting from Jerusalem artichoke (1.1 wt%), sorghum (2.6 wt%), miscanthus (1.1 wt%), foxtail millet (1.5 wt%) and *Arundo donax* (1.6 wt%) in the presence of NbPO, ~~and of the same order of magnitude with that reached by us only after 1 h of reaction~~ starting from sorghum (1.6 wt%) in the presence of ZrPO. Finally, in all runs reported in Tables 9 and 10 the %C recovered (mol%) underlines~~both for hemicellulose and cellulose for both catalytic systems and for all the real investigated biomasses underlines~~ the moderate presence of humins, which anyway is higher for NbPO than ZrPO.

In conclusion, starting from raw lignocellulosic biomasses, NbPO and ZrPO enable us to achieve high percentages of hemicellulose and cellulose solubilization and~~,~~ hydrolysates rich in hemicellulose and cellulose sugars and oligomers to be further valorized. In particular, ~~and~~ starting from Jerusalem artichoke, in the presence of ~~niobium~~ NbPO and ~~zirconium phosphate~~ZrPO respectively, yields to furanic compounds of 12.7 mol% and to ~~cellulose~~ cellulose-derived sugars of 50.0 mol% were achieved after only 1 h of reaction, thus confirming their high potential as heterogeneous acid catalysts in biomass conversion.

As previously reported, NbPO and ZrPO showed high stability and ~~an~~ easy recyclability when employed in the glucose conversion. However, in order to demonstrate the real feasibility of their employment also in the conversion of real feedstocks, their recyclability was further investigated, in particular for Jerusalem artichoke, the most promising biomass. In this case, the solids recovered at the end of the catalytic reactions contained not only the spent catalyst but also the unconverted biomass, thus ~~resulting~~making more

complex the separation of the catalyst from the substrate and its recyclinge ~~more complex~~. For this purpose, the solid residues recovered from the hydrolysis of Jerusalem artichoke with NbPO and ZrPO were thermally treated at 500 °C for 5 h with the aim of burning the unconverted biomass and recovering the catalysts, which are stable at this temperature, as demonstrated by the TGA (Figure 6). The post-treated NbPO and ZrPO~~as recovered~~ catalysts were subsequently employed ~~in~~within other two recycleing runs, under the same reaction conditions of the first one (150 °C, autogenic pressure, 1 h). Regarding the conversion of Jerusalem artichoke hemicellulose fraction, both recycled catalysts ~~led in the recycle runs the same results previously achieved in the first one~~gave analogous results to the first run (results are not shown), whereas some differences were observed in the conversion of cellulose fraction, as shown in Figure 11.

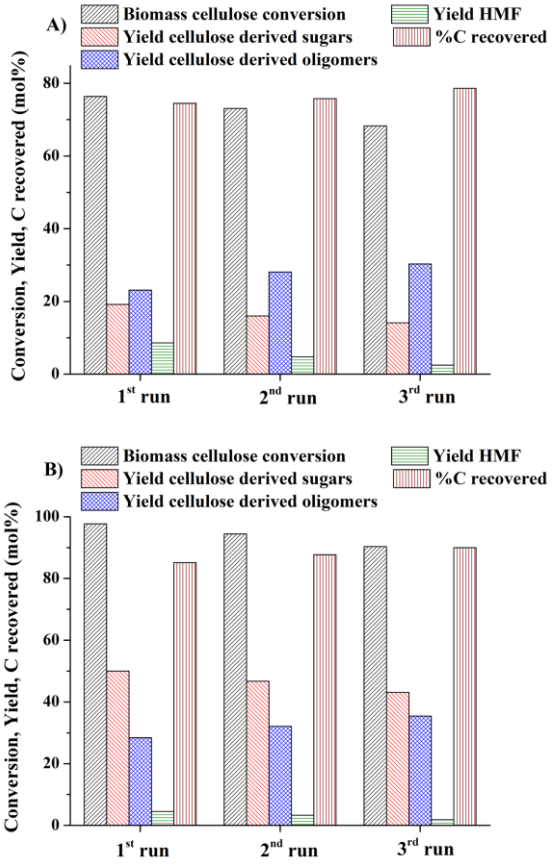

Figure 11: Conversion of Jerusalem artichoke cellulosic fraction in the recycle runs of: A) NbPO and B) ZrPO at 150 °C. Reaction conditions: biomass = 2.68 g catalysts = 2.23 g water = 51.0 g T = 150 °C, autogenic pressure, 1 h. As reported in the Materials and Methods, yields have been calculated with respect to the amount of cellulose or hemicellulose present in the starting biomass.

The results further confirmed that the hydrolysis of hemicellulose was easier than that of cellulose and a not relevant deactivation of the catalysts during their recycle did not affect its conversion. On the other hand, the slight deactivation of both catalysts caused ~~the~~a little decrease of cellulose conversion, together with the decrease of HMF and sugars yields and the increase of oligomers one, being the hydrolysis of cellulose partly limited by the slight lost of catalytic activity. In particular, after the third recycleing run of NbPO, the cellulose conversion, sugar yield and HMF yield decreased from 76.4, 19.2 and 8.6 mol% to 68.3, 14.1 and 2.5 mol%, respectively, in favor of the oligomers formation that achieved the yield of 30.3 mol% from 23.1 mol% (Figure 11A). Regarding ZrPO, after the third recycle run, the cellulose conversion moderately decreased to 94.4 mol% from

97.7 mol%, analogously to sugars and HMF yields that lowered from 50.0 and 4.5 mol% to 43.1 and 1.8 mol%, respectively, whereas the oligomers yield raised to 35.4 mol% from 28.4 mol% (Figure 11B). In conclusion, the thermal treatment of the solid residues recovered at the end of the process represents an efficient strategy for the removal of unconverted biomass and allows the successful recycle of the catalysts that ~~showed to~~ maintain almost unchanged their starting catalytic activity.

3. Materials and Methods

3.1 Materials

Glucose, xylose, fructose, levulinic acid and furfural were purchased by Sigma-Aldrich (Sigma-Aldrich, St. Louis, MO, USA) and used as-received. 5-hydroxymethtylfurfural was supplied by AVA Biochem (AVA Biochem AG, Zug, Switzerland). NbPO was kindly provided from CBMM (Companhia Brasileira de Metalurgia e Mineracão, Araxá, Minas Gerais, Brasil). It was~~,~~ calcined in static air at 400 °C for 3 h with a heating rate of 10°C/min before its use. ZrPO was prepared according to the procedure reported by Kamiya et al. [40~~68~~~~75~~]. In particular, two different solutions were prepared in two different beakers by dissolving 10.5 g of $ZrOCl_2 \cdot 8H_2O$ in 32 mL of distilled water (1 M) and 7.4 g of $NH_4H_2PO_4$ in 64 mL of water (1 M), respectively. The latter solution was added dropwise, under magnetic stirring (600 rpm), to the first beaker at room temperature without any other expedients, obtaining the precipitation of a white solid characterized by a P/Zr atomic ratio equal to 2. ~~through the precipitation of $ZrOCl_2 \cdot 8H_2O$ (32 mL of 1 M aqueous solution) and $NH_4H_2PO_4$ (64 mL of a 1 M solution), at a molar ratio of P/Zr = 2.~~ The precipitate was then filtered, washed with distilled water, dried at 100 °C and finally calcined in static air at 400 °C for 3 h with a heating rate of 10 °C/min before its use. Microcrystalline cellulose Avicel PH-101 (particle size 50 µm) was purchased by Sigma-Aldrich (Sigma-Aldrich, St. Louis, MO, USA) and used as-received, whereas the ball-milled sample was achieved after a treatment in a tungsten carbide vial for 48 h. Lignocellulosic waste biomasses, namely conifer wood sawdust, Jerusalem artichoke, sorghum, miscanthus, foxtail millet, hemp and *Arundo donax*, were provided by Prof. Monti and Prof. Zanetti of the Agriculture School of the University of Bologna. All biomasses were dried and ball milled for 15 minutes ~~e~~ before ~~employed for~~ the catalytic tests ~~they have been ball milled for 15 minutes.~~

3.2 Catalytic reactions

The conversion tests of glucose, cellulose and real lignocellulosic biomasses (conifer wood sawdust, Jerusalem artichoke, sorghum, miscanthus, foxtail millet, hemp and *Arundo donax*) were performed in autoclave adopting a 300 mL mechanically stirred Parr 4560 reactor (Parr Instrument Company, Moline, IL, USA), equipped with a P.I.D. controller 4843, an electrical heating system, temperature and stirring control devices. In a typical procedure, the desired amount of the catalyst, substrate and water were placed in the reactor, which was then subjected to repeated cycles of evacuation and nitrogen flushing to ensure the complete oxygen removal. Isothermal conditions were maintained for the desired reaction time. In each experiment, time zero was taken at the beginning of the isothermal stage. Reaction mixture samples were periodically withdrawn through the sampling valve during the reaction, quickly cooled and ~~analysed~~analyzed by HPLC. At the end of the reaction, the mixture was cooled, collected in water and then filtered over a Buchner filter. After the filtration, the solid residue was recovered, dried overnight at 80°C in an oven, and then analyzed to determine the conversion of the biomass substrate. Each test was performed in triplicate.

Glucose conversion reactions were also performed in a monomodal microwave reactor CEM Discover S-class System (CEM Corporation, Matthews, NC, USA). In a standard reaction, the feedstock was charged in the microwave (MW) reactor (10 mL) with the

proper amount of the catalyst. The vessel was placed in the chamber of the MW reactor and heated up to reachat the desired temperature for the selected time under magnetic stirring. At the end of the reaction, the vessel was cooled at room temperature through an external air flow that allows a fast cooling and a portion of the sample was taken for the analysis. Each test was performed in triplicate.

HPCL HPLC analyses were carried out using an Agilent 1260 Infinity Series HPLC system (Agilent Technologies, Santa Clara, CA, USA), equipped with a manual injector with a 20 µL calibrated loop equipped with two different columns. The quantification of monosaccharides was performed by using an Agilent Hi-Plex Pb column (Agilent Technologies, Santa Clara, CA, USA) (length=30 cm, diameter=7.7 mm, particle size=8 µm), whose stationary phase was made of a divinylbenzene-styrene copolymer functionalized with Pb^{2+} ions. The column was thermostated at 80 °C and 0.6 mL/min flow of water was used as eluent. The detection of products occurreds by means of a refraction index detector (RID), thermostated at 40 °C. On the other hand, the quantification of organic acids and furans was carried out adopting a Phenomenex Rezex ROA-H column (Phenomenex, Torrance, CA, USA) (length=30 cm, diameter=7.7 mm, particle size=8 µm), whose stationary phase was made of a divinylbenzene-styrene copolymer functionalized with H^+ ions. The column was thermostated at 60 °C and 0.6 mL/min flow of 0.0025 M H_2SO4 solution was used as eluent. The detection of products occurredoccurs by means of a UV-diode array detector (UV-DAD), recording the absorbance at 253, 205 and, 192 nm.

The oOligomers quantification and the analysis of the chemical composition of both starting raw biomasses and treated residues as well as lignocellulose biomasses and residues compositions were evaluated following the standard procedure of Sluiter et al. [416976].

The catalytic performances werehave been reported in terms of conversion, selectivity and yield. These latterand were calculated on molar basis, considering glucose or the anhydroglucose unit offor cellulose. In the following equations, for the sake of simplicity, glucose was has been always reported as reference.

Glucose conversion (mol%) = [(moles glucose in − moles glucose out)/moles glucose in] x 100;

Selectivity to compound i (mol%) = [(moles compound i)/(moles glucose in − moles glucose out)] x 100;

Yield to compound i (mol%) = (moles compound i/moles glucose in) x 100.

For lignocellulosic biomasses, catalytic performances werehave been also expressed in terms of molar basis, adopting the Sluiter protocol for the quantification of oligomers [618]. In particular, the conversion of cellulose and hemicellulose conversions, together with the yields ofto sugars (glucose and fructose) and to oligomers coming from cellulose, the yields ofto sugars (xylose, arabinose, galactose and mannose) and to oligomers coming from hemicellulose, the HMF yield (deriving from cellulose) and the furfural yield (deriving from hemicellulose) were considered and calculated according to the following equations.

Biomass cellulose conversion (mol%) = [(moles anhydroglucose cellulose in − moles anhydroglucose residue out)/moles anhydroglucose cellulose in] x 100;

Biomass hemicellulose conversion (mol%) = [(moles anhydroxylose hemicellulose in − moles anhydroxylose residue out)/moles anhydroxylose hemicellulose in] x 100;

Yield to Ccellulose derived sugars yield (mol%) = [(moles glucose + moles fructose)/(moles anhydroglucose cellulose in)] x 100;

Yield to Ccellulose-derive oligomers yield (mol%) = [(moles glucose out post Sluiter − moles glucose out post reaction)/moles anhydroglucose cellulose in] x 100;

Yield to Hhemicellulose derived sugars yield (mol%) = [(moles xylose + moles arabinose + moles galactose + moles mannose)/(moles anhydroxylose hemicellulose in)] x 100;

Yield to Hhemicellulose-derived oligomers yield (mol%) = [(moles xylose out post Sluiter − moles xylose out post reaction)/moles anhydroxylose hemicellulose in] x 100;

~~Yield to~~ HMF yield (mol%) = [(moles HMF)/(moles anhydroglucose cellulose in)] x 100;

~~Yield to f~~Furfural yield (mol%) = [(moles furfural)/(moles anhydroxylose hemicellulose in)] x 100.

The %C recovered~~carbon balance~~ was evaluated as the sum of the moles of products and moles of unconverted reagent (glucose and/or anhydrosugars for cellulose and real biomasses) with respect to the initial moles of reagent (glucose and/or anhydrosugars for cellulose and real biomasses), expressed in mol%.

All the experiments were carried out in triplicate and the reproducibility of the technique was within 5%.

The catalysts employed in the conversion of Jerusalem artichoke were separated from the unconverted biomass through thermal treatment that allowed the combustion of the organic matter. This thermal treatment was performed in a muffle furnace Nabertherm L 9/11/SKM/P330 (Nabertherm, Lilienthal, Germany) at 500 °C for 5 h.

3.3 Analysis of catalyst properties

The main characterization of fresh NbPO and ZrPO was~~has been~~ reported in our previous work [2~~6~~].

XRD analyses were carried out using a vertical goniometer diffractometer Philips PW 1050/81 (Philips, Amsterdam, The Netherlands). The analyses were performed using the CuK radiation, which was made monochromatic by using a nickel filter, with λ=0.15418 nm. The adopted interval ~~used~~ was $5° < 2\theta < 80°$, with steps of 0.2°; the count of intensity was carried out every 2 s.

FT-IR analyses were recorded in ATR mode with a Spectrum Two Perkin Elmer FT-IR spectrometer (Perkin Elmer, Waltham, MA, USA) in the range of wavenumber 4000-450 cm^{-1}.

TGA analyses were performed by using a TGA Q500 instrument (TA Instruments, New Castle, DE, USA) in the temperature range of 30-800 °C, at a heating rate of 10°C/min, and under an air flow of 20 mL/min.

Scanning electron microscopy associated with an energy dispersion spectrometry (SEM/EDS) analysis was performed with JEOL -6010/LA microscope (JEOL Ltd., Tokyo, Japan). The EDS spectra were obtained using a working distance of 10 mm and a voltage of 20 KV. The crystal structure of the catalyst was evaluated by a Bruker model D8 X-ray diffractometer (Bruker, Billerica, MA, USA) discovered under Cu Kα (λ=0.15441 nm) in the 2θ range of 5-80° at a scan rate of 3°/min.

XRF analyses were performed employing a wavelength dispersive spectrometer Panalytical Axios Advanced (Malvern Panalytical, Malvern, UK) equipped with tube rhodium and characterized by ~~with~~ a power of 4 kW.

Nitrogen adsorption/desorption isotherms (77 K) were recorded at -196°C using a Micromeritics ASAP 2020 instrument (Micromeritics, Norcross, GA, USA). Samples were previously outgassed for 120 minutes at 423 K and 30 μmHg and then heated for 240 minutes at 623 K. Specific surface area values were obtained by using the multi-point BET equation in the 0.05-0.2 p/p0 range and total pore volume values were calculated at 0.95 p/p0.

4. Conclusions

In this work, niobium and zirconium phosphates were~~have been~~ tested as heterogeneous acid catalysts for the hydrothermal conversion of glucose, cellulose and ~~of~~ six strategic lignocellulosic biomasses, produced as agricultural and forestry residues, such as

conifer wood sawdust, Jerusalem artichoke, sorghum, miscanthus, foxtail millet, hemp and *Arundo donax*. Among the available heterogeneous acid catalysts, metal phosphates result very promising, due to their high thermal stability and good water-tolerance. The HMF yield of 24.4 mol% and the LA yield of 24.0 mol% were achieved starting from model compounds ~~In particular, starting from model compounds, good yields to HMF (24.4 mol%) and LA (24.0 mol%) have been achieved~~ using ~~respectively~~ niobium and zirconium phosphates at 160 and 180 °C, respectively. On the other hand, when real lignocellulosic biomasses were employed as the substrate~~have been studied~~, both catalysts fostered the hemicellulose and cellulose solubilization. In particular, starting from Jerusalem artichoke, miscanthus and foxtail millet, ~~hydrolysates~~hydrolyzates~~,~~ rich in C5 and C6 sugars and oligomers~~,~~ were ~~have been~~ produced~~.~~ ~~,~~ These hydrolyzates ~~which~~ can be further valorized towards the production of a wide range of bio-based ~~to a plethora of~~ compounds through catalytic and/or biocatalytic conversion cascade processes. ~~I~~Moreover, ~~in more detail,~~ ~~–Z~~zirconium phosphate ~~ZrPO~~ promoted~~s~~ the hydrolysis of the starting biomasses~~,~~ causing a higher production of monosaccharides from cellulose and hemicellulose, such as glucose and fructose from the cellulose fraction, and xylose, arabinose, galactose and mannose from the hemicellulose one.~~,~~ Differently,~~whereas~~ niobium phosphate ~~NbPO~~ was~~results~~ active towards the sugars consecutive products derived from C5 and C6, such as furfural and HMF~~, respectively~~. In particular, s~~S~~tarting from Jerusalem artichoke, the yield of furanic compounds was 12.7 mol% while the yield of cellulose-derived sugars was 50.0 mol% in the presence of niobium and zirconium phosphate, respectively, ~~in the presence of NbPO niobium and ZrPO zirconium phosphate, respectively, yields to furanic compounds of 12.7 mol% and to cellulose derived sugars of 50.0 mol% were obtained~~ after only 1 h of reaction, adopting the biomass/catalyst weight ratio of 1.2, thus resulting a promising starting feedstock, moving towards heterogeneously catalyzed biomass conversion. These ~~behaviours~~behaviors were ~~have been~~ related to the acid properties of the proposed catalysts, in particular the total acidity, the Brønsted/Lewis acid sites ratio and their strength, giving us the opportunity to better tune the reaction towards the target product/s.

Author Contributions: Conceptualization, C.A., A.M.R.G. and F.C.; methodology, C.A., A.M.R.G., A.M. and F.C.; formal analysis, C.A., D.L., S.F., N.D.F., F.Z. and T.T.; writing—original draft preparation, C.A., D.L. and T.T.; writing—review and editing, C.A., A.M.R.G., A.M. and F.C.; supervision, C.A., A.M.R.G. and F.C. All authors have read and agreed to the published version of the manuscript.

Acknowledgments: The authors are grateful to Italian Ministero dell'Istruzione dell'Università e della Ricerca for the financial support provided through the PRIN 2020 LEVANTE project "LEvulinic acid Valorization through Advanced Novel Technologies" (Progetti di Ricerca di Rilevante Interesse Nazionale -Bando 2020, 2020CZCJN7).

Conflicts of Interest: The authors declare no conflict of interest.

References

1. Xu, H.; Li, X.; Hu, W.; Lu, L.; Chen, J.; Zhu, Y.; Zhou, H.; Si, C. Recent advances on solid acid catalytic systems for production of 5-hydroxymethylfurfural from biomass derivatives. *Fuel Process. Technol.* **2022**, *234*, 107338-107356; DOI:10.1016/j.fuproc.2022.107338.
2. Antonetti, C.; Melloni, M.; Licursi, D.; Fulignati, S.; Ribechini, E.; Rivas, S.; Parajó, J.C.; Cavani, F.; Raspolli Galletti, A.M. Microwave-assisted dehydration of fructose and inulin to HMF catalyzed by niobium and zirconium phosphate catalysts. *Appl. Catal. B: Environ.* **2017**, *206*, 364-377, DOI:10.1016/j.apcatb.2017.01.056.
3. Azlan, N.S.M.; Yap, C.L.; Gan, S.; Rahman, M.B.A. Recent advances in the conversion of lignocellulosic biomass and its degraded products to levulinic acid: A synergy of Brønsted-Lowry acid and Lewis acid. *Ind. Crops Prod.* **2022**, *181*, 114778-114802; DOI:10.1016/j.indcrop.2022.114778.

4. Antonetti, C.; Licursi, D.; Fulignati, S.; Valentini, G.; Raspolli Galletti, A.M. New frontiers in the catalytic synthesis of levulinic acid: from sugars to raw and waste biomass as starting feedstock. *Catalysts* **2016**, *6*, 196-224; DOI:10.3390/catal6120196.
5. Messori, A.; Fasolini, A.; Mazzoni, R. Advances in Catalytic Routes for the homogeneous green conversion of the bio-based platform 5-hydroxymethylfurfural. *ChemSusChem* **2022**, *15*, 202200228-202200245; DOI:10.1002/cssc.202200228.
6. Rivas, S.; Raspolli Galletti, A.M.; Antonetti, C.; Licursi, D.; Santos, V.; Parajó, J.C. A biorefinery cascade conversion of hemicellulose-free *Eucalyptus globulus* wood: production of concentrated levulinic acid solutions for γ-valerolactone sustainable preparation. *Catalysts* **2018**, *8*, 169-184; DOI:10.3390/catal8040169.
7. Fulignati, S.; Antonetti, C.; Wilbers, E.; Licursi, D.; Heeres, H.J.; Raspolli Galletti, A.M. Tunable HMF hydrogenation to furan diols in a flow reactor using Ru/C as catalyst. *J. Ind. Eng. Chem.* **2021**, *100*, 390.e1-390.e9; DOI:10.1016/j.jiec.2021.04.057
8. Xu, W.P.; Chen, X.F.; Guo, H.J.; Li, H.L.; Zhang, H.R.; Xiong, L.; Chen, X.D.; Biotechnology. Conversion of levulinic acid to valuable chemicals: a review. *J. Chem. Technol. Biotechnol.* **2021**, *96*, 3009-3024; DOI:10.1002/jctb.6810.
9. Shi, N.; Liu, Q.; Cen, H.; Ju, R.; He, X.; Ma, L. Formation of humins during degradation of carbohydrates and furfural derivatives in various solvents. *Biomass Convers. Biorefinery* **2020**, *10*, 277-287; DOI:10.1007/s13399-019-00414-4.
10. Shi, N.; Liu, Q.; Ju, R.; He, X.; Zhang, Y.; Tang, S.; Ma, L. Condensation of α-carbonyl aldehydes leads to the formation of solid humins during the hydrothermal degradation of carbohydrates. *ACS Omega* **2019**, *4*, 7330-7343; DOI:10.1021/acsomega.9b00508.
11. Deng, L.; Li, J.; Lai, D.M.; Fu, Y.; Guo, Q.X. Catalytic conversion of biomass-derived carbohydrates into γ-valerolactone without using an external H_2 supply. *Angew. Chem. Int. Ed.* **2009**, *121*, 6651-6654; DOI:10.1002/ange.200902281.
12. Flannelly, T.; Lopes, M.; Kupiainen, L.; Dooley, S.; Leahy, J. Non-stoichiometric formation of formic and levulinic acids from the hydrolysis of biomass derived hexose carbohydrates. *RSC Adv.* **2016**, *6*, 5797-5804; DOI:10.1039/C5RA25172A.
13. Acharjee, T.C.; Lee, Y.Y. Production of levulinic acid from glucose by dual solid-acid catalysts. *Environ. Prog. Sustain. Energy* **2018**, *37*, 471-480; DOI:10.1002/ep.12659.
14. Weingarten, R.; Kim, Y.T.; Tompsett, G.A.; Fernández, A.; Han, K.S.; Hagaman, E.W.; Conner Jr, W.C.; Dumesic, J.A.; Huber, G.W. Conversion of glucose into levulinic acid with solid metal (IV) phosphate catalysts. *J. Catal.* **2013**, *304*, 123-134; DOI:10.1016/j.jcat.2013.03.023.
15. Marianou, A.A.; Michailof, C.M.; Pineda, A.; Iliopoulou, E.; Triantafyllidis, K.; Lappas, A. Effect of Lewis and Brønsted acidity on glucose conversion to 5-HMF and lactic acid in aqueous and organic media. *Appl. Catal. A: Gen.* **2018**, *555*, 75-87; DOI:10.1016/j.apcata.2018.01.029.
16. Wang, K.; Liang, C.; Zhang, Q.; Zhang, F. Synergistic catalysis of Brønsted acid and Lewis acid coexisted on ordered mesoporous resin for one-pot conversion of glucose to 5-hydroxymethylfurfural. *ACS Omega* **2019**, *4*, 1053-1059; DOI:10.1021/acsomega.8b02982.
17. Krawielitzki, S. AVA Biochem, Pioneer in industrial biobased furan chemistry. *Chimia* **2020**, *74*, 776-778; DOI:10.2533/chimia.2020.776.
18. Hu, D.; Zhang, M.; Xu, H.; Wang, Y.; Yan, K. Recent advance on the catalytic system for efficient production of biomass-derived 5-hydroxymethylfurfural. *Renewable and Sustainable Energy Reviews* **2021**, *147*, 111253; DOI:10.1016/j.rser.2021.111253.
19. Villa, A.; Schiavoni, M.; Fulvio, P.F.; Mahurin, S.M.; Dai, S.; Mayes, R.T.; Veith, G.M.; Prati, L. Phosphorylated mesoporous carbon as effective catalyst for the selective fructose dehydration to HMF. *J. Energy Chem.* **2013**, *22*, 305-311; DOI:10.1016/S2095-4956(13)60037-6.
20. Van der Graaf, W.N.P.; Tempelman, C.H.L.; Hendriks, F.C.; Ruiz-Martinez, J.; Bals, S.; Weckhuysen, B.M.; Pidko, E.A.; Hensen, E.J.M. Deactivation of Sn-Beta during carbohydrate conversion. *Appl. Catal. A Gen.* **2018**, *564*, 113-122; DOI:10.1016/j.apcata.2018.07.023.
21. Oozeerally, R.; Burnett, D.L.; Chamberlain, T.W.; Kashtiban, R.J.; Huband, S.; Walton, R.I.; Degirmenci, V. Systematic modification of UiO-66 metal-organic frameworks for glucose conversion into 5-hydroxymethyl furfural in water. *ChemCatchem* **2021**, *13*, 2517-2529; DOI:10.1002/cctc.202001989.
22. Wang, K.X.; Liang, C.; Zhang, Q.X.; Zhang, F. Synergistic catalysis of Bronsted acid and Lewis acid coexisted on ordered mesoporous resin for one-pot conversion of glucose to 5-hydroxymethylfurfural. *ACS Omega* **2019**, *4*, 1053.1059; DOI:10.1021/acsomega.8b02982.
23. Zhang, Y.; Wang, J.; Li, X.; Liu, X.; Xia, Y.; Hu, B.; Lu, G.; Wang, Y. Direct conversion of biomass-derived carbohydrates to 5-hydroxymethylfurural over water-tolerant niobium-based catalysts. *Fuel* **2015**, *139*, 301-307; DOI:10.1016/j.fuel.2014.08.047.
24. De Jesus Junior, M.M.; Fernandes, S.A.; Borges, E.; Baêta, B.E.L.; De Ávila Rodrigues, F. Kinetic study of the conversion of glucose to 5-hydroxymethylfurfural using niobium phosphate. *Mol. Catal.* **2022**, *518*, 112079-112088; DOI:10.1016/j.mcat.2021.112079.
25. Ordomsky, V.; Sushkevich, V.; Schouten, J.; Van Der Schaaf, J.; Nijhuis, T. Glucose dehydration to 5-hydroxymethylfurfural over phosphate catalysts. *J. Catal.* **2013**, *300*, 37-46; DOI:10.1016/j.jcat.2012.12.028.
26. Liu, Q.; Liu, H.; Gao, D.M. Establishing a kinetic model of biomass-derived disaccharide hydrolysis over solid acid: a case study on hierarchically porous niobium phosphate. *Chem. Eng. J.* **2022**, *430*, 132756-132765; DOI:10.1016/j.cej.2021.132756.
27. Saravanan, K.; Park, K.S.; Jeon, S.; Bae, J.W. Aqueous phase synthesis of 5-hydroxymethylfurfural from glucose over large pore mesoporous zirconium phosphates: effect of calcination temperature. *ACS Omega* **2018**, *3*, 808-820; DOI:10.1021/acsomega.7b01357.

28. Parshetti, G.K.; Suryadharma, M.S.; Pham, T.P.T.; Mahmood, R.; Balasubramanian, R. Heterogeneous catalyst-assisted thermo-chemical conversion of food waste biomass into 5-hydroxymethylfurfural. *Bioresour. Technol.* **2015**, *178*, 19-27; DOI:10.1016/j.biortech.2014.10.066.
29. Vieira, J.L.; Paul, G.; Iga, G.D.; Cabral, N.M.; Bueno, J.M.C.; Bisio, C.; Gallo, J.M.R. Niobium phosphates as bifunctional catalysts for the conversion of biomass-derived monosaccharides. *Appl. Catal. A: Gen.* **2021**, *617*, 118099-118109; DOI:10.1016/j.apcata.2021.118099.
30. Antonetti, C.; Gori, S.; Licursi, D.; Pasini, G.; Frigo, S.; López, M.; Parajó, J.C.; Raspolli Galletti, A.M. One-pot alcoholysis of the lignocellulosic *Eucalyptus nitens* biomass to *n*-butyl levulinate, a valuable additive for diesel motor fuel. *Catalysts* **2020**, *10*, 509-530; DOI:10.3390/catal10050509.
31. Tatzber, M.; Stemmer, M.; Spiegel, H.; Katzlberger, C.; Haberhauer, G.; Mentler, A.; Gerzabek, M.H. FTIR-spectroscopic characterization of humic acids and humin fractions obtained by advanced NaOH, $Na_4P_2O_7$, and Na_2CO_3 extraction procedures. *J. Plant Nutr. Soil Sci.* **2007**, *170*, 522-529; DOI:10.1002/jpln.200622082.
32. Patil, S.K.; Lund, C.R. Formation and growth of humins via aldol addition and condensation during acid-catalyzed conversion of 5-hydroxymethylfurfural. *Energy Fuels* **2011**, *25*, 4745-4755; DOI:10.1021/ef2010157.
33. Carniti, P.; Gervasini, A.; Bossola, F.; Dal Santo, V. Cooperative action of Brønsted and Lewis acid sites of niobium phosphate catalysts for cellobiose conversion in water. *Appl. Catal. B: Environ.* **2016**, *193*, 93-102; DOI:10.1016/j.apcatb.2016.04.012.
34. Sing, K.S.W.; Everett, D.H.; Haul, R.A.W.; Moscou, R.A.; Pierotti, R.; Rouquerol, J.; Siemieniewska, T. Reporting physisorption data for gas/solid systems. In *Handbook of heterogeneous catalysis*, 1st ed.; Wiley-VCH Verlag GmbH & Co: Weinheim, Germany, 2008; Volume 1, pp. 1217-1230; DOI:10.1351/pac198557040603.
35. Gliozzi, G.; Innorta, A.; Mancini, A.; Bortolo, R.; Perego, C.; Ricci, M.; Cavani, F. Zr/P/O catalyst for the direct acid chemo-hydrolysis of non-pretreated microcrystalline cellulose and softwood sawdust. *Appl. Catal. B: Environ.* **2014**, *145*, 24-33; DOI:10.1016/j.apcatb.2012.12.035.
36. Shimizu, K.; Furukawa, H.; Kobayashi, N.; Itaya, Y.; Satsuma, A. Effects of Brønsted and Lewis acidities on activity and selectivity of heteropolyacid-based catalysts for hydrolysis of cellobiose and cellulose. *Green Chem.* **2009**, *11*, 1627-1632; DOI:10.1039/B913737H.
37. Di Fidio, N.; Raspolli Galletti, A.M.; Fulignati, S.; Licursi, D.; Liuzzi, F.; De Bari, I.; Antonetti, C. Multi-Step exploitation of raw *Arundo donax* L. for the selective synthesis of second-generation sugars by chemical and biological route. *Catalysts* **2020**, *10*, 79-101; DOI:10.3390/catal10010079.
38. Di Fidio, N.; Ragaglini, G.; Dragoni, F.; Antonetti, C.; Raspolli Galletti, A.M. Integrated cascade biorefinery processes for the production of single cell oil by *Lipomyces starkeyi* from *Arundo donax* L. hydrolysates. *Bioresource Technology* **2021**, *325*, 124635; DOI:10.1016/j.biortech.2020.124635.
39. Zhang, Z.; Zhu, Z.; Shen, B.; Liu, L. Insights into biochar and hydrochar production and applications: A review. *Energy* **2019**, *171*, 581-598; DOI:10.1016/j.energy.2019.01.035.
40. Kamiya, Y.; Sakata, S.; Yoshinaga, Y.; Ohnishi, R.; Okuhara, T. Zirconium phosphate with a high surface area as a water-tolerant solid acid. *Catal. Lett.* **2004**, *94*, 45-47; DOI:10.1023/B:CATL.0000019329.82828.e4.
41. Sluiter, A.; Hames, B.; Ruiz, R.; Scarlata, C.; Sluiter, J.; Templeton, D.; Crocker, D. *Determination of structural carbohydrates and lignin in biomass.* NREL/TP-510-42618; National Renewable Energy Laboratory: Golden, CO, USA 2008, 1617, 1-16.

~~1. Xu, H.; Li, X.; Hu, W.; Lu, L.; Chen, J.; Zhu, Y.; Zhou, H.; Si, C. Recent advances on solid acid catalytic systems for production of 5-hydroxymethylfurfural from biomass derivatives. *Fuel Process. Technol.* **2022**, *234*, 107338-107356; DOI:10.1016/j.fuproc.2022.107338.~~
~~2. Rani, M.A.A.B.A.; Karim, N.A.; Kamarudin, S.K. Microporous and mesoporous structure catalysts for the production of 5-hydroxymethylfurfural (5-HMF). *Int. J. Energy Res.* **2022**, *46*, 577-633; DOI:10.1002/er.7247.~~
~~3. Iris, K.M.; Tsang, D.C.W. Conversion of biomass to hydroxymethylfurfural: a review of catalytic systems and underlying mechanisms. *Bioresour. Technol.* **2017**, *238*, 716-732; DOI:10.1016/j.biortech.2017.04.026.~~
~~4. Agarwal, B.; Kailasam, K.; Sangwan, R.S.; Elumalai, S. Traversing the history of solid catalysts for heterogeneous synthesis of 5-hydroxymethylfurfural from carbohydrate sugars: A review. *Renew. Sustain. Energy Rev.* **2018**, *82*, 2408-2425; DOI:10.1016/j.rser.2017.08.088.~~
~~5. Antonetti, C.; Raspolli Galletti, A.M.; Fulignati, S.; Licursi, D. Amberlyst A-70: A surprisingly active catalyst for the MW-assisted dehydration of fructose and inulin to HMF in water. *Catal. Commun.* **2017**, *97*, 146-150; DOI:10.1016/j.catcom.2017.04.032.~~
~~6. Antonetti, C.; Melloni, M.; Licursi, D.; Fulignati, S.; Ribechini, E.; Rivas, S.; Parajó, J.C.; Cavani, F.; Raspolli Galletti, A.M. Microwave-assisted dehydration of fructose and inulin to HMF catalyzed by niobium and zirconium phosphate catalysts. *Appl. Catal. B: Environ.* **2017**, *206*, 364-377, DOI:10.1016/j.apcatb.2017.01.056.~~
~~7. Antonetti, C.; Fulignati, S.; Licursi, D.; Raspolli Galletti, A.M. Turning point toward the sustainable production of 5-hydroxymethyl-2-furaldehyde in water: Metal salts for its synthesis from fructose and inulin. *ACS Sustain. Chem. Eng.* **2019**, *7*, 6830-6838; DOI:10.1021/acssuschemeng.8b06162.~~
~~8. Azlan, N.S.M.; Yap, C.L.; Can, S.; Rahman, M.B.A. Recent advances in the conversion of lignocellulosic biomass and its degraded products to levulinic acid: A synergy of Brønsted-Lowry acid and Lewis acid. *Ind. Crops Prod.* **2022**, *181*, 114778-114802; DOI:10.1016/j.indcrop.2022.114778.~~

9. Sajid, M.; Farooq, U.; Bary, G.; Azim, M.M.; Zhao, X. Sustainable production of levulinic acid and its derivatives for fuel additives and chemicals: progress, challenges, and prospects. *Green Chem.* **2021**, *23*, 9198–9238; DOI:10.1039/D1GC02919C.
10. Liu, C.; Lu, X.; Yu, Z.; Xiong, J.; Bai, H.; Zhang, R. Production of levulinic acid from cellulose and cellulosic biomass in different catalytic systems. *Catalysts* **2020**, *10*, 1006–1027; DOI:10.3390/catal10091006.
11. Kang, S.; Fu, J.; Zhang, G. From lignocellulosic biomass to levulinic acid: A review on acid-catalyzed hydrolysis. *Renew. Sustain. Energy Rev.* **2018**, *94*, 340–362; DOI:10.1016/j.rser.2018.06.016.
12. Antonetti, C.; Licursi, D.; Fulignati, S.; Valentini, G.; Raspolli Galletti, A.M. New frontiers in the catalytic synthesis of levulinic acid: from sugars to raw and waste biomass as starting feedstock. *Catalysts* **2016**, *6*, 196–224; DOI:10.3390/catal6120196.
13. Girisuta, B.; Heeres, H.J. Levulinic acid from biomass: Synthesis and applications. In *Production of platform chemicals from sustainable resources*, 1st ed.; Fang, Z., Smith, Jr., R., Qi, X., Ed.; Springer: Singapore, 2017; Volume 1, pp. 143–169; DOI:10.1007/978-981-10-4172-3_5.
14. Antonetti, C.; Bonari, E.; Licursi, D.; Nassi o Di Nasso, N.; Raspolli Galletti, A.M. Hydrothermal conversion of giant reed to furfural and levulinic acid: optimization of the process under microwave irradiation and investigation of distinctive agronomic parameters. *Molecules* **2015**, *20*, 21232–21253; DOI:10.3390/molecules201219760.
15. Messori, A.; Fasolini, A.; Mazzoni, R. Advances in Catalytic Routes for the homogeneous green conversion of the bio-based platform 5-hydroxymethylfurfural. *ChemSusChem* **2022**, *15*, 202200228–202200245; DOI:10.1002/cssc.202200228.
16. Iriondo, A.; Agirre, I.; Viar, N.; Requies, J. Value added bio-chemicals commodities from catalytic conversion of biomass derived furan compounds. *Catalysts* **2020**, *10*, 895–917; DOI:10.3390/catal10080895.
17. Fulignati, S.; Antonetti, C.; Wilbers, E.; Licursi, D.; Heeres, H.J.; Raspolli Galletti, A.M. Tunable HMF hydrogenation to furandiols in a flow reactor using Ru/C as catalyst. *J. Ind. Eng. Chem.* **2021**, *100*, 390.e1–390.e9; DOI:10.1016/j.jiec.2021.04.057
18. Xu, W.P.; Chen, X.F.; Guo, H.J.; Li, H.L.; Zhang, H.R.; Xiong, L.; Chen, X.D.; Biotechnology. Conversion of levulinic acid to valuable chemicals: a review. *J. Chem. Technol. Biotechnol.* **2021**, *96*, 3009–3024; DOI:10.1002/jctb.6810.
19. Rivas, S.; Raspolli Galletti, A.M.; Antonetti, C.; Licursi, D.; Santos, V.; Parajó, J.C. A biorefinery cascade conversion of hemicellulose-free *Eucalyptus globulus* wood: production of concentrated levulinic acid solutions for γ-valerolactone sustainable preparation. *Catalysts* **2018**, *8*, 169–184; DOI:10.3390/catal8040169.
20. Licursi, D.; Antonetti, C.; Fulignati, S.; Giannoni, M.; Raspolli Galletti, A.M. Cascade strategy for the tunable catalytic valorization of levulinic acid and γ-valerolactone to 2-methyltetrahydrofuran and alcohols. *Catalysts* **2018**, *8*, 277–292; DOI:10.3390/catal8070277.
21. Vásquez, P.B.; Tabanelli, T.; Monti, E.; Albonetti, S.; Bonincontro, D.; Dimitratos, N.; Cavani, F. Gas-phase catalytic transfer hydrogenation of methyl levulinate with ethanol over ZrO_2. *ACS Sustain. Chem. Eng.* **2019**, *7*, 8317–8330; DOI:10.1021/acssuschemeng.8b06744.
22. Bellè, A.; Tabanelli, T.; Fiorani, G.; Perosa, A.; Cavani, F.; Selva, M. A multiphase protocol for selective hydrogenation and reductive amination of levulinic acid with integrated catalyst recovery. *ChemSusChem* **2019**, *12*, 3343–3354; DOI:10.1002/cssc.201900925.
23. Van Zandvoort, I.; Wang, Y.; Rasrendra, C.B.; Van Eck, E.R.; Bruijnincx, P.C.; Heeres, H.J.; Weckhuysen, B.M. Formation, molecular structure, and morphology of humins in biomass conversion: influence of feedstock and processing conditions. *ChemSusChem* **2013**, *6*, 1745–1758; DOI:10.1002/cssc.201300332.
24. Shi, N.; Liu, Q.; Cen, H.; Ju, R.; He, X.; Ma, L. Formation of humins during degradation of carbohydrates and furfural derivatives in various solvents. *Biomass Convers. Biorefinery* **2020**, *10*, 277–287; DOI:10.1007/s13399-019-00414-4.
25. Shi, N.; Liu, Q.; Ju, R.; He, X.; Zhang, Y.; Tang, S.; Ma, L. Condensation of α-carbonyl aldehydes leads to the formation of solid humins during the hydrothermal degradation of carbohydrates. *ACS Omega* **2019**, *4*, 7330–7343; DOI:10.1021/acsomega.9b00508.
26. Deng, L.; Li, J.; Lai, D.M.; Fu, Y.; Guo, Q.X. Catalytic conversion of biomass-derived carbohydrates into γ-valerolactone without using an external H_2 supply. *Angew. Chem. Int. Ed.* **2009**, *121*, 6651–6654; DOI:10.1002/ange.200902281.
27. Flannelly, T.; Lopes, M.; Kupiainen, L.; Dooley, S.; Leahy, J. Non-stoichiometric formation of formic and levulinic acids from the hydrolysis of biomass derived hexose carbohydrates. *RSC Adv.* **2016**, *6*, 5797–5804; DOI:10.1039/C5RA25172A.
28. Choudhary, V.; Mushrif, S.H.; Ho, C.; Anderko, A.; Nikolakis, V.; Marinkovic, N.S.; Frenkel, A.I.; Sandler, S.I.; Vlachos, D.G. Insights into the interplay of Lewis and Brønsted acid catalysts in glucose and fructose conversion to 5-(hydroxymethyl) furfural and levulinic acid in aqueous media. *J. Am. Chem. Soc.* **2013**, *135*, 3997–4006; DOI:10.1021/ja3122763.
29. Acharjee, T.C.; Lee, Y.Y. Production of levulinic acid from glucose by dual solid acid catalysts. *Environ. Prog. Sustain. Energy* **2018**, *37*, 471–480; DOI:10.1002/ep.12659.
30. Jiang, L.; Zhou, L.; Chao, J.; Zhao, H.; Lu, T.; Su, Y.; Yang, X.; Xu, J. Direct catalytic conversion of carbohydrates to methyl levulinate: synergy of solid Brønsted acid and Lewis acid. *Appl. Catal. B: Environ.* **2018**, *220*, 589–596; DOI:10.1016/j.apcatb.2017.08.072.
31. Boonyakarn, T.; Wataniyakul, P.; Boonnoun, P.; Quitain, A.T.; Kida, T.; Sasaki, M.; Laosiripojana, N.; Jongsomjit, B.; Shotipruk, A. Enhanced levulinic acid production from cellulose by combined Brønsted hydrothermal carbon and Lewis acid catalysts. *Ind. Eng. Chem. Res.* **2019**, *58*, 2697–2703; DOI:10.1021/acs.iecr.8b05332.
32. Weingarten, R.; Kim, Y.T.; Tompsett, G.A.; Fernández, A.; Han, K.S.; Hagaman, E.W.; Conner Jr, W.C.; Dumesic, J.A.; Huber, G.W. Conversion of glucose into levulinic acid with solid metal (IV) phosphate catalysts. *J. Catal.* **2013**, *304*, 123–134; DOI:10.1016/j.jcat.2013.03.023.

33. Swift, T.D.; Nguyen, H.; Erdman, Z.; Kruger, J.S.; Nikolakis, V.; Vlachos, D.G. Tandem Lewis acid/Brønsted acid catalyzed conversion of carbohydrates to 5-hydroxymethylfurfural using zeolite beta. *J. Catal.* **2016**, *333*, 149-161; DOI:10.1016/j.jcat.2015.10.009.
34. Marianou, A.A.; Michailof, C.M.; Pineda, A.; Iliopoulou, E.; Triantafyllidis, K.; Lappas, A. Effect of Lewis and Brønsted acidity on glucose conversion to 5-HMF and lactic acid in aqueous and organic media. *Appl. Catal. A: Gen.* **2018**, *555*, 75-87; DOI:10.1016/j.apcata.2018.01.029.
35. Wang, K.; Liang, C.; Zhang, Q.; Zhang, F. Synergistic catalysis of Brønsted acid and Lewis acid coexisted on ordered mesoporous resin for one-pot conversion of glucose to 5-hydroxymethylfurfural. *ACS Omega* **2019**, *4*, 1053-1059; DOI:10.1021/acsomega.8b02982.
36. Krawielitzki, S. AVA Biochem, Pioneer in industrial biobased furan chemistry. *Chimia* **2020**, *74*, 776-778; DOI:10.2533/chimia.2020.776.
37. Hu, D.; Zhang, M.; Xu, H.; Wang, Y.; Yan, K. Recent advance on the catalytic system for efficient production of biomass-derived 5-hydroxymethylfurfural. *Renewable and Sustainable Energy Reviews* **2021**, *147*, 111253; DOI:10.1016/j.rser.2021.111253.
38. Villa, A.; Schiavoni, M.; Fulvio, P.F.; Mahurin, S.M.; Dai, S.; Mayes, R.T.; Veith, G.M.; Prati, L. Phosphorylated mesoporous carbon as effective catalyst for the selective fructose dehydration to HMF. *J. Energy Chem.* **2013**, 22, 305-311; DOI:10.1016/S2095-4956(13)60037-6.
39. Van der Graaf, W.N.P.; Tempelman, C.H.L.; Hendriks, F.C.; Ruiz-Martinez, J.; Bals, S.; Weckhuysen, B.M.; Pidko, E.A.; Hensen, E.J.M. Deactivation of Sn-Beta during carbohydrate conversion. *Appl. Catal. A Gen.* **2018**, *564*, 113-122; DOI:10.1016/j.apcata.2018.07.023.
40. Oozeerally, R.; Burnett, D.L.; Chamberlain, T.W.; Kashtiban, R.J.; Huband, S.; Walton, R.I.; Degirmenci, V. Systematic modification of UiO-66 metal-organic frameworks for glucose conversion into 5-hydroxymethyl furfural in water. *ChemCatchem* **2021**, *13*, 2517-2529; DOI:10.1002/cctc.202001989.
41. Wang, K.X.; Liang, C.; Zhang, Q.X.; Zhang, F. Synergistic catalysis of Bronsted acid and Lewis acid coexisted on ordered mesoporous resin for one-pot conversion of glucose to 5-hydroxymethylfurfural. *ACS Omega* **2019**, *4*, 1053.1059; DOI:10.1021/acsomega.8b02982.
42. De Jesus Junior, M.M.; Fernandes, S.A.; Borges, E.; Baêta, B.E.L.; De Ávila Rodrigues, F. Kinetic study of the conversion of glucose to 5-hydroxymethylfurfural using niobium phosphate. *Mol. Catal.* **2022**, *518*, 112079-112088; DOI:10.1016/j.mcat.2021.112079.
43. Liu, Q.; Liu, H.; Gao, D.M. Establishing a kinetic model of biomass-derived disaccharide hydrolysis over solid acid: a case study on hierarchically porous niobium phosphate. *Chem. Eng. J.* **2022**, *430*, 132756-132765; DOI:10.1016/j.cej.2021.132756.
44. Vieira, J.L.; Paul, G.; Iga, G.D.; Cabral, N.M.; Bueno, J.M.C.; Bisio, C.; Gallo, J.M.R. Niobium phosphates as bifunctional catalysts for the conversion of biomass-derived monosaccharides. *Appl. Catal. A: Gen.* **2021**, *617*, 118099-118109; DOI:10.1016/j.apcata.2021.118099.
45. Li, N.; Xu, M.; Wang, N.; Shen, Q.; Wang, K.; Zhou, J. Preparation of 5-hydroxymethylfurfural from cellulose catalyzed by chemical bond anchoring catalyst $Hf_xZr_{1-x}P/SiO_2$. *React. Kinet. Mech. Catal.* **2021**, *133*, 157-171; DOI:10.1007/s11144-021-01989-8.
46. Campisi, S.; Bennici, S.; Auroux, A.; Carniti, P.; Gervasini, A. A rational revisiting of niobium oxophosphate catalysts for carbohydrate biomass reactions. *Top. Catal.* **2018**, *61*, 1939-1948; DOI:10.1007/s11244-018-0999-x.
47. De Carvalho, E.G.; Rodrigues, F.d.A.; Monteiro, R.S.; Ribas, R.M.; Da Silva, M. Experimental design and economic analysis of 5-hydroxymethylfurfural synthesis from fructose in acetone-water system using niobium phosphate as catalyst. *Biomass Convers. Biorefin.* **2018**, *8*, 635-646; DOI:10.1007/s13399-018-0319-5.
48. Ni, W.; Li, D.; Zhao, X.; Ma, W.; Kong, K.; Gu, Q.; Chen, M.; Hou, Z. Catalytic dehydration of sorbitol and fructose by acid-modified zirconium phosphate. *Catal. Today* **2019**, *319*, 66-75; DOI:10.1016/j.cattod.2018.03.034.
49. Zhu, C.; Cai, C.; Liu, Q.; Li, W.; Tan, J.; Wang, C.; Chen, L.; Zhang, Q.; Ma, L. Continuous production of 5-hydroxymethylfurfural from monosaccharide over zirconium phosphates. *ChemistrySelect* **2018**, *3*, 10983-10990; DOI:10.1002/slct.201801880.
50. Villanueva, N.I.; Marzialetti, T.G. Mechanism and kinetic parameters of glucose and fructose dehydration to 5-hydroxymethylfurfural over solid phosphate catalysts in water. *Catal. Today* **2018**, *302*, 100-107; DOI:10.1016/j.cattod.2017.04.049.
51. Zhang, Y.; Wang, J.; Li, X.; Liu, X.; Xia, Y.; Hu, B.; Lu, G.; Wang, Y. Direct conversion of biomass-derived carbohydrates to 5-hydroxymethylfurural over water-tolerant niobium-based catalysts. *Fuel* **2015**, *139*, 301-307; DOI:10.1016/j.fuel.2014.08.047.
52. Jain, A.; Shore, A.M.; Jonnalagadda, S.C.; Ramanujachary, K.V.; Mugweru, A. Conversion of fructose, glucose and sucrose to 5-hydroxymethyl-2-furfural over mesoporous zirconium phosphate catalyst. *Appl. Catal. A: Gen.* **2015**, *489*, 72-76; DOI:10.1016/j.apcata.2014.10.020.
53. Ordomsky, V.; Sushkevich, V.; Schouten, J.; Van Der Schaaf, J.; Nijhuis, T. Glucose dehydration to 5-hydroxymethylfurfural over phosphate catalysts. *J. Catal.* **2013**, *300*, 37-46; DOI:10.1016/j.jcat.2012.12.028.
54. Saravanan, K.; Park, K.S.; Jeon, S.; Bae, J.W. Aqueous phase synthesis of 5-hydroxymethylfurfural from glucose over large pore mesoporous zirconium phosphates: effect of calcination temperature. *ACS Omega* **2018**, *3*, 808-820; DOI:10.1021/acsomega.7b01357.
55. Parshetti, G.K.; Suryadharma, M.S.; Pham, T.P.T.; Mahmood, R.; Balasubramanian, R. Heterogeneous catalyst-assisted thermochemical conversion of food waste biomass into 5-hydroxymethylfurfural. *Bioresour. Technol.* **2015**, *178*, 19-27; DOI:10.1016/j.biortech.2014.10.066.

56. Upare, P.P.; Yoon, J.W.; Kim, M.Y.; Kang, H.Y.; Hwang, D.W.; Hwang, Y.K.; Kung, H.H.; Chang, J.S. Chemical conversion of biomass-derived hexose sugars to levulinic acid over sulfonic acid-functionalized graphene oxide catalysts. *Green Chem.* **2013**, *15*, 2935-2943; DOI:10.1039/C3GC40353J.
57. Ramli, N.A.S.; Amin, N.A.S. Kinetic study of glucose conversion to levulinic acid over Fe/HY zeolite catalyst. *Chem. Eng. J.* **2016**, *283*, 150-159; DOI:10.1016/j.cej.2015.07.044.
58. Tang, P.; Yu, J. Kinetic analysis on deactivation of a solid Brønsted acid catalyst in conversion of sucrose to levulinic acid. *Ind. Eng. Chem. Res.* **2014**, *53*, 11629-11637; DOI:10.1021/ie501044c.
59. Yu, F.; Thomas, J.; Smet, M.; Dehaen, W.; Sels, B.F. Molecular design of sulfonated hyperbranched poly(arylene oxindole)s for efficient cellulose conversion to levulinic acid. *Green Chem.* **2016**, *18*, 1694-1705; DOI:10.1039/C5GC01971K.
60. Joshi, S.S.; Zodge, A.D.; Pandare, K.V.; Kulkarni, B.D. Efficient conversion of cellulose to levulinic acid by hydrothermal treatment using zirconium dioxide as a recyclable solid acid catalyst. *Ind. Eng. Chem. Res.* **2014**, *53*, 18796-18805; DOI:10.1021/ie5011838.
61. Zuo, Y.; Zhang, Y.; Fu, Y. Catalytic conversion of cellulose into levulinic acid by a sulfonated chloromethyl polystyrene solid acid catalyst. *ChemCatChem* **2014**, *6*, 753-757; DOI:10.1002/cctc.201300956.
62. Potvin, J.; Sorlien, E.; Hegner, J.; DeBoef, B.; Lucht, B.L. Effect of NaCl on the conversion of cellulose to glucose and levulinic acid via solid supported acid catalysis. *Tetrahedron Lett.* **2011**, *52*, 5891-5893; DOI:10.1016/j.tetlet.2011.09.013.
63. Kammoun, M.; Istasse, T.; Ayeb, H.; Rassaa, N.; Bettaieb, T.; Richel, A. Hydrothermal dehydration of monosaccharides promoted by seawater: fundamentals on the catalytic role of inorganic salts. *Front. Chem.* **2019**, *7*, 132-143; DOI:10.3389/fchem.2019.00132.
64. Hegner, J.; Pereira, K.C.; DeBoef, B.; Lucht, B.L. Conversion of cellulose to glucose and levulinic acid via solid-supported acid catalysis. *Tetrahedron Lett.* **2010**, *51*, 2256-2258; DOI:10.1016/j.tetlet.2010.02.145.
65. Antonetti, C.; Gori, S.; Licursi, D.; Pasini, G.; Frigo, S.; López, M.; Parajó, J.C.; Raspolli Galletti, A.M. One-pot alcoholysis of the lignocellulosic *Eucalyptus nitens* biomass to *n*-butyl levulinate, a valuable additive for diesel motor fuel. *Catalysts* **2020**, *10*, 509-530; DOI:10.3390/catal10050509.
66. Tatzber, M.; Stemmer, M.; Spiegel, H.; Katzlberger, C.; Haberhauer, G.; Mentler, A.; Gerzabek, M.H. FTIR-spectroscopic characterization of humic acids and humin fractions obtained by advanced NaOH, $Na_4P_2O_7$, and Na_2CO_3 extraction procedures. *J. Plant Nutr. Soil Sci.* **2007**, *170*, 522-529; DOI:10.1002/jpln.200622082.
67. Patil, S.K.; Lund, C.R. Formation and growth of humins via aldol addition and condensation during acid-catalyzed conversion of 5-hydroxymethylfurfural. *Energy Fuels* **2011**, *25*, 4745-4755; DOI:10.1021/ef2010157.
68. Carniti, P.; Gervasini, A.; Bossola, F.; Dal Santo, V. Cooperative action of Brønsted and Lewis acid sites of niobium phosphate catalysts for cellobiose conversion in water. *Appl. Catal. B: Environ.* **2016**, *193*, 93-102; DOI:10.1016/j.apcatb.2016.04.012.
69. Sing, K.S.W.; Everett, D.H.; Haul, R.A.W.; Moscou, R.A.; Pierotti, R.; Rouquerol, J.; Siemieniewska, T. Reporting physisorption data for gas/solid systems. In *Handbook of heterogeneous catalysis*, 1st ed.; Wiley-VCH Verlag GmbH & Co: Weinheim, Germany, 2008; Volume 1, pp. 1217-1230; DOI:10.1351/pac198557040603.
70. Gliozzi, G.; Innorta, A.; Mancini, A.; Bortolo, R.; Perego, C.; Ricci, M.; Cavani, F. Zr/P/O catalyst for the direct acid-chemohydrolysis of non-pretreated microcrystalline cellulose and softwood sawdust. *Appl. Catal. B: Environ.* **2014**, *145*, 24-33; DOI:10.1016/j.apcatb.2012.12.035.
71. Shimizu, K.; Furukawa, H.; Kobayashi, N.; Itaya, Y.; Satsuma, A. Effects of Brønsted and Lewis acidities on activity and selectivity of heteropolyacid-based catalysts for hydrolysis of cellobiose and cellulose. *Green Chem.* **2009**, *11*, 1627-1632; DOI:10.1039/B913737H.
72. Di Fidio, N.; Raspolli Galletti, A.M.; Fulignati, S.; Licursi, D.; Liuzzi, F.; De Bari, I.; Antonetti, C. Multi-Step exploitation of raw *Arundo donax* L. for the selective synthesis of second-generation sugars by chemical and biological route. *Catalysts* **2020**, *10*, 79-101; DOI:10.3390/catal10010079.
73. Di Fidio, N.; Ragaglini, G.; Dragoni, F.; Antonetti, C.; Raspolli Galletti, A.M. Integrated cascade biorefinery processes for the production of single cell oil by *Lipomyces starkeyi* from *Arundo donax* L. hydrolysates. *Bioresource Technology* **2021**, *325*, 124635; DOI:10.1016/j.biortech.2020.124635.
74. Zhang, Z.; Zhu, Z.; Shen, B.; Liu, L. Insights into biochar and hydrochar production and applications: A review. *Energy* **2019**, *171*, 581-598; DOI:10.1016/j.energy.2019.01.035.
75. Kamiya, Y.; Sakata, S.; Yoshinaga, Y.; Ohnishi, R.; Okuhara, T. Zirconium phosphate with a high surface area as a water-tolerant solid acid. *Catal. Lett.* **2004**, *94*, 45-47; DOI:10.1023/B:CATL.0000019329.82828.e4.
76. Sluiter, A.; Hames, B.; Ruiz, R.; Scarlata, C.; Sluiter, J.; Templeton, D.; Crocker, D. *Determination of structural carbohydrates and lignin in biomass.* NREL/TP-510-42618; National Renewable Energy Laboratory: Golden, CO, USA 2008, 1617, 1-16.